

Investigating the role of nuclear lamins in regulating the stemness and neuronal differentiation of NT2/D1 embryonal carcinoma cells

A thesis

submitted in partial fulfilment of the requirements
for the degree of Masters in Science

By

Saswati Kar

(Reg. ID: 20192007)

Under the guidance of

Dr Kundan Sengupta



INDIAN INSTITUTE OF SCIENCE EDUCATION AND RESEARCH, PUNE

April 2022


© Saswati Kar 2022

All rights reserved

Certificate

This is to certify that this dissertation entitled “Investigating the role of nuclear lamins in regulating the stemness and neuronal differentiation of NT2/D1 embryonal carcinoma cells” submitted towards the partial fulfilment of the 3-years MS with research degree programme at the Indian Institute of Science Education and Research, Pune represents the study/work carried out by Saswati Kar under the supervision of Dr Kundan Sengupta, Associate Professor, Department of Biology, during the academic year 2021-2022.

Supervisor


14.06.2022
डॉ. कुंदन सेनगुप्ता / Dr. Kundan Sengupta
आसोसो प्रोफेसर / Associate Professor
बायोलॉजी विभाग / Department of Biology
Indian Institute of Science Education & Research
पुणे / Pune - 411 008, India

Dr Kundan Sengupta

Committee:

Dr Kundan Sengupta

Dr Mridula Nambiar

Dr Aurnab Ghose

Dr Thomas Pucadyil

This thesis is dedicated to my parents and my sister, whose unwavering support has constantly motivated me to challenge myself, tackle every obstacle and strive forward.

Declaration

I hereby declare that the matter embodied in the report entitled “Investigating the role of nuclear lamins in regulating the stemness and neuronal differentiation of NT2/D1 embryonal carcinoma cells” are the results of the work carried out by me at the Department of Biology, Indian Institute of Science Education and Research, Pune, under the supervision of Dr Kundan Sengupta and the same has not been submitted elsewhere for any other degree.

Saswati Kar

Saswati Kar

Date: 30.04.2022

Table of Contents

Abstract.....	6
Acknowledgements.....	7
Introduction.....	8
Materials and Methods.....	12
Results.....	24
Discussion.....	37
Conclusion.....	39
Future perspectives.....	39
References.....	40
Extended Methods.....	44
Extended Results.....	45

List of Tables

Table 1: List of primers used for RT-qPCR.....	14
Table 2: List of primary antibodies used for IFA.....	17
Table 3: List of siRNA oligonucleotides used for transfection.....	18
Table 4: List of primary antibodies used for western blotting.....	19

List of Figures

Figure 1: Understanding of the role of nuclear lamins in regulating cell fate changes.....	11
Figure 2: Workflow of lamin quantification from IFA.....	20
Figure 3: Pipeline for 3' mRNA sequencing.....	23
Figure 4: Workflow of differential gene expression analysis using Bluebee.....	24
Figure 5: RA-mediated differentiation of NT2/D1 cells.....	26
Figure 6: Changes in lamins transcript levels during NT2/D1 differentiation.....	28
Figure 7: Regulation of stemness in NT2/D1 by lamins.....	30
Figure 8: Co-regulatory roles of lamin subtypes.....	31
Figure 9: Differentiation in cells with depleted lamins.....	33
Figure 10: Possible cross-talk between lamins and NUP93-complex.....	35
Figure 11: Differentiation in cells with depleted NUP205.....	37
Figure 12: Network analyses of lamin-nucleoporins interaction.....	39
Figure E1: Karyotypic validation of NT2/D1 cells.....	46
Figure E2: Expression changes in relevant nuclear proteins during differentiation.....	47
Figure E3: Interaction network mapping of nuclear envelope proteins with PCGs.....	48

Abstract

Cells undergo transition in lineages from one cell type to another with extensive rearrangement of their transcriptomic signatures. This is made possible by facilitating changes in their genomic and nuclear architecture, largely brought about by major nuclear envelope proteins, including lamins and nucleoporins. Lamins are filamentous proteins that provide structural integrity to the nucleus and also regulate chromatin architecture and gene expression. Cellular differentiation of pluripotent NT2/D1 cells into specialised neuronal cells serves as a good model to study the mechanistic roles of the different lamin subtypes in regulating the highly dynamic processes involved in cell fate transition. In this study, the three lamin subtypes- A, B1 and B2, in association with proteins of the nucleoporin-93 subcomplex, have been shown to play a significant role in distinctly modulating the stemness of the pluripotent NT2/D1 cells, as well as differentially regulating the initiation and progression of differentiation of these cells along the neuronal lineage in a temporal manner. We have speculated that the lamins facilitate this cellular differentiation by directly impacting the gene expression of certain pluripotency and differentiation-specific factors.

Acknowledgements

I would like to thank Dr Kundan Sengupta for giving me an opportunity to pursue an independent research project in his lab and for his invaluable guidance and encouragement throughout this project. I am grateful to the members of the Chromosome Biology Lab for their support, help, discussions, and critical review of my work.

I would also like to thank my colleagues Gargee Joshi and Jayati Khanna, and my collaborators Dr Ajay Labade, Adwait Salvi and Jiffin Benjamin for their help with designing and conducting the experiments for this project. I also thank my Research Advisory committee members, Dr Mridula Nambiar, Dr Aurnab Ghose, Dr Dimple Notani, and Dr Krishanpal Karmodiya, for their insights and suggestions.

I would like to acknowledge IISER Pune for my funding during this project. I would also like to express my gratitude to the IISER Pune microscopy facility, NGS facility and proteomics facility for their assistance while generating and analysing the data for this project. I thank all members of the IISER Pune Biology department for their prompt help and advice whenever required, especially to the members of Galande lab, Karmodiya lab and Kamat lab.

I express my heartfelt thanks to all my batchmates (Integrated PhD Biology, batch of 2019) for being my pillars of strength and motivation throughout my academic and research experience at IISER Pune. Lastly, I thank my family for their support and motivation every step of the way.

1. Introduction

Every cell type has a unique transcriptional and proteomic profile that bestows it with a specific cellular identity. This distinct profiling is largely a read-out of the pre-defined chromosomal and nucleosomal arrangement within the nucleus of a cell, particularly in eukaryotic cells. The nuclear membrane is known to be primarily responsible for the compartmentalisation of the genomic material from the cytoplasm in a cell (Lusk and King, 2017). Apart from bestowing mechanical support to the nucleus (Agrawal and Lele, 2019) and allowing for the nucleo-cytoplasmic exchange of materials (McPherson et al., 2015), literature over the past decade has increasingly shown that the components of the nuclear envelope also play a significant role in regulating gene expression. In some cases, the nuclear envelope proteins like the lamins directly associate with the chromatin and determine their arrangement and gene transcription (Briand and Collas, 2020), while in other cases, these proteins indirectly regulate the expression of other transcription factors (Andrés and González, 2009; Dorner et al., 2007) and signalling molecules (Marmioli et al., 2009, Andrés and González, 2009). This process is highly dynamic in nature, especially in the case of pluripotent cells. The pluripotent cells are naive or unspecialised cells with a poised chromatin architecture (Crispatzu et al., 2021; Ikeda et al., 2017) and have the ability to differentiate into many different cell types with varied lineages and specialisations. These cellular differentiation processes have been observed to be driven by specific changes in their gene expression profiles (Zhou et al., 2020; Zhang et al., 2019) that are closely associated with modifications in their nuclear structure (Heo et al., 2016).

A number of different cell lines can be externally induced to undergo differentiation into cells of specific lineages by administering appropriate differentiation agents *in vitro*. Traditionally, embryonic stem cells (ESCs) or induced pluripotent stem cells (iPSCs) have been used to study the behaviour and differentiation of pluripotent cells (Marei et al., 2017). However, a group of stem cell-like transformed cell lines also exists, referred to as the testicular germ cell (TGC) lines. Being cancerous in nature, these cells exhibit erratic activation of certain cellular and molecular pathways, developing a heterogeneous population of malignant tumours called teratocarcinoma (Rapley et al., 2009). These tumours have a considerable population of undifferentiated cells exhibiting the histological features of primordial germ cells (PGCs) that can be differentiated into specialised cells (Rapley et al., 2009). Since these undifferentiated populations of cells are pluripotent in nature and can differentiate and develop into different germ layers, thus recapitulating the early developmental events like the ESCs, they are referred to as embryonal carcinoma (EC) cells (Kleinsmith and Pierce, 1964). ECs being tumorigenic in nature, show high proliferative ability and are easier to grow and culture than ESCs and iPSCs, making them a suitable *in vitro* differentiation model. NTERA-2 cl.D1 (NT2/D1) is an EC line commonly used to study cellular differentiation by the administration of differentiation-inducer agents (Pleasure and Lee, 1993). Administration of Bone Morphogenetic Proteins (BMP-2/BMP-7) to the NT2/D1 cells differentiates them along a majorly epithelial lineage (Chadalavada et al., 2005; Caricasole et al., 2000), while

trans-retinoic acid (RA) treatment induces differentiation in these cells along a neuro-ectodermal lineage (Coyle et al., 2011; Baldassarre et al., 2000).

RA is a retinol (vitamin A) derived metabolite that acts as an active morphogen during embryonic development by binding to nuclear receptors called the retinoic acid receptors (RARs) of the retinoid receptor family of proteins (Rochette-Egly, 2015). RARs (type α , β , and γ) are transcription factors, which upon binding to RA, form heterodimers with retinoid X receptors (RXRs) (le Maire et al., 2019). This dimeric complex then binds to the specific DNA sequences called the retinoic acid response elements (RAREs) present in the promoter regions of genes necessary for differentiation, thus activating their expression (le Maire et al., 2019) and inducing developmental changes in the cell and nucleus towards a neuronal phenotype. Ideally, 10 μ M RA is potent to terminally differentiate the NT2/D1 cells into the post-mitotic stage of neurons after a course of 21 days of daily treatment (Coyle et al., 2011). Since this study focuses more on observing the progression of differentiation rather than on a post-differentiated system, we have considered a period of 8-10 days of RA treatment suitable for our experimental observations since the majority of the population of cells are understood to have differentiated beyond pluripotency or multipotency by this time.

The nuclear envelope in a cell is double-membranous, comprising a number of proteins in the outer and inner nuclear membrane. Lamins are an integral component of the nuclear membrane. They are type V intermediate filament proteins that form a meshwork towards the nucleoplasmic side of the inner nuclear membrane, serving as a major mechanical support for the nuclear shape and structure (Patil and Sengupta, 2021), as well as a scaffold for chromatin organisation and gene expression (Smith et al., 2021). There are two broad categories of lamins: A-type and B-type lamins. In humans, A-type lamins are transcribed by the *LMNA* gene, producing two major splice variants, Lamin A and Lamin C. On the other hand, the B-type lamin genes *LMNB1* and *LMNB2* code for two independent proteins, Lamin B1 and Lamin B2 respectively (Patil and Sengupta, 2021). Since the cell, as well as the nucleus, undergoes significant rearrangement during changes in the cell fate, driving it from one cell type to another, nuclear lamins expression and localisation are generally altered in the process (Heo et al., 2016). Moreover, lamins have also been known to actively regulate cell fate transitions like cellular differentiation in pluripotent cells (Alcorta-Sevillano et al., 2020; Heo et al., 2016). The *LMNA* gene promoter exhibits RARE elements, and the expression of Lamin A/C is directly activated by RA (Okumura et al., 2000). Although Lamin A has been extensively studied in the context of cellular differentiation and development, recent studies have revealed crucial roles of B-type lamins in influencing these processes (Bedrosian et al., 2021; Yattah et al., 2020; Mahajani et al., 2017). In this study, the effect of A-type lamins and B-type lamins has been studied independently but simultaneously in order to observe potential co-regulatory and combinatorial effects of their expression on the initiation and progression of differentiation in NT2/D1 cells (Fig.1). For this study, lamin subtypes have been referred to as Lamin A, Lamin B1 and Lamin B2 encoded by *LMNA*, *LMNB1* and *LMNB2* genes respectively. However, the other splice variants of the *LMNA* gene products are promising molecules whose role could be explored further.

Like lamins, nucleoporins (Nups) are also a component of the nuclear membrane which form the subunits of different multi-protein complexes called the nuclear pore complex (NPC) that aid in the nucleo-cytoplasmic exchange of proteins and RNA ([Raices and D'Angelo, 2022](#)). Apart from their canonical function in nuclear transport, recent studies have also implicated the role of Nups in gene expression regulation ([Sumner and Brickner, 2022](#); [Khan et al., 2020](#)). For instance, in a previous study, we found that the NUP93 protein of the NUP93-NPC actively regulates the gene localisation and expression of the critical developmental factor *HOXA* during RA-differentiation of NT2/D1 cells in a spatio-temporal manner ([Labade et al., 2021](#)). It is worthwhile to investigate the role of the other proteins in the NUP93-complex, majorly NUP188 and NUP205, in regulating this process. Being proximal to the nuclear lamins, the role of NUP93-complex proteins in maintaining and regulating the differentiability of NT2/D1 cells has been briefly investigated along with lamins in this study to probe for possible mechanistic cross-talk between the two families of the nuclear membrane proteins.

Figure 1

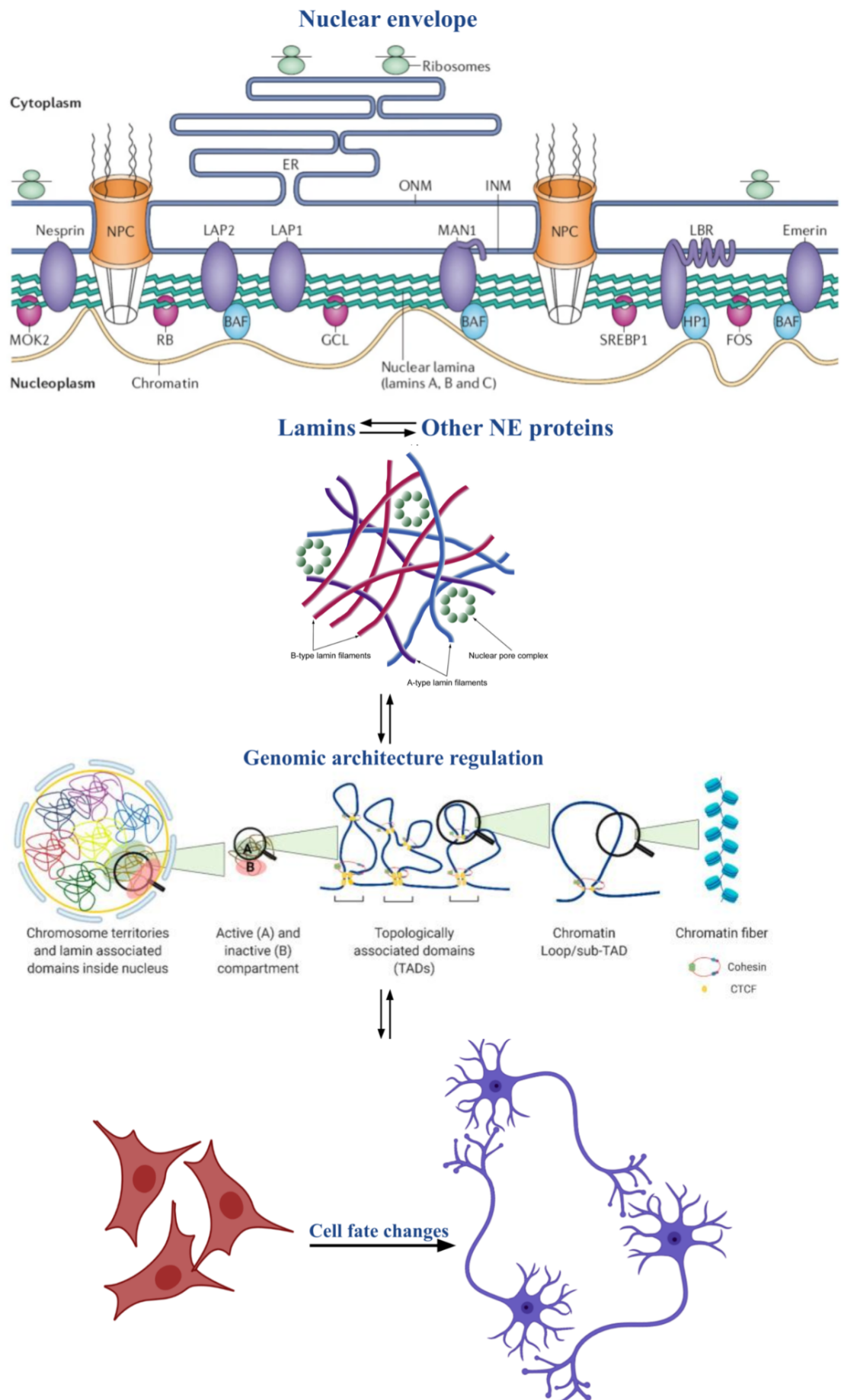


Fig. 1: Conceptual understanding of the role of nuclear lamins in regulating cell fate transitions. Representative image to show the role of lamins in re-organising genomic architecture via modulation of transcription factor expression, signalling molecules, and epigenetic remodelers to facilitate cell fate changes. [The images have been modified from [Alps et al., 2021](#); [Xie et al., 2016](#); and [Coutinho et al., 2009](#)].

2. Materials and Methods

2.1 Cell culture

2.1.1 Revival: The NT2/D1 (NTERA-2 cl. D1) cell line was generously provided by the lab of Dr Sanjeev Galande (IISER Pune, India) with permission from Dr Peter Andrews (The University of Sheffield, UK). The cells were revived in Dulbecco's Modified Eagle's medium (DMEM; Gibco, 11995) supplemented with 20% fetal bovine serum (FBS; Sigma-Aldrich, F2442), 100 U/ml Penicillin-Streptomycin (Gibco, 15070063), and 2 mM L-glutamine (GlutaMAX; Gibco, 35050061) in a sterile incubator set at 37 °C and 5% CO₂.

2.1.2 Maintenance: The cultures were maintained in complete DMEM with 10% FBS at a minimum confluence of 30% at all times.

2.1.3 Passaging: Confluent cells were passaged by treating them with 0.05% Trypsin-EDTA (Gibco, 25300062) dissociation agent (~1 ml for a 100 mm culture dish) for 2-5 minutes, and trypsinisation was stopped by adding 2X volume of the complete medium as that of trypsin. The dissociated cells were thoroughly mixed to ensure a suspension of isolated cells and were centrifuged at 1,000 rpm for 5-10 minutes at 10 °C. The pellet was then re-suspended in fresh culture medium and divided into passaged populations in the ratio of 1:2 or 1:3.

2.1.4 Preservation: The cells were stored for long-term use by cryo-preserving them in a freezing medium of 9:1 FBS:DMSO. Actively dividing cells were harvested at a 70-80% confluence and counted using a hemocytometer. 1-2 million cells were suspended in 1 ml of freezing medium per cryo-vial and gradually frozen at a rate of -1 °C/min in an iso-propanol chamber and then shifted to -80°C or liquid nitrogen after 24-48 hours.

2.2 Karyotyping

The NT2/D1 cells were arrested at the metaphase stage of their cell division cycle by treating the cultures with 0.1 µg/ml Colcemid (Roche, 10295892001) for 90 minutes at 37 °C and 5% CO₂. The cells were harvested by trypsinisation, washed with 1X PBS and spun down to a pellet. The cells were then treated with a hypotonic solution (0.075 M KCl) for 30 minutes, followed by fixation using 4–5 drops of the fixative (3:1 Methanol:Acetic Acid). The fixed cells were then centrifuged at 1,000 rpm for 10 minutes at 4 °C. The cells were then washed thrice with the fixative solution by suspending the pellet in the fixative solution at an appropriate dilution. Finally, the cells were dropped onto clean, humidified glass slides. The dropped metaphases were then stained with DAPI solution (0.05 µg/ml in 1X PBS) and observed under a fluorescence microscope. The number of chromosomes (modal number) in

each metaphase was counted and plotted against the frequency of occurrence of the modal number in order to validate the cell line.

2.3 RA-mediated cell differentiation

10 mM RA stock was prepared by dissolving the powder (Sigma-Aldrich, R2625) in DMSO and was stored at -80°C in amber tubes with 1 ml aliquots, protected from light. While in use, the aliquot was stored at -20°C and used within 1 week. The cultures were grown in a reduced serum medium (5% FBS in complete DMEM) to facilitate differentiation by uptake of RA. A regular pulse of 10 μM RA was provided in fresh medium every 24-48 hours to initiate differentiation in the NT2/D1 cells towards a neuroectodermal lineage. Ideally, 8 days of RA administration has been referred to as a complete treatment for differentiation for this project, unless mentioned otherwise. Adequate care was taken to avoid exposing the cultures to direct light sources since RA degrades when exposed to light.

2.4 RNA isolation and complementary DNA synthesis

The adherent cells or harvested suspension of cells were washed with 1X PBS to remove all traces of media. A guanidinium thiocyanate based lysis reagent like TRIzol (Invitrogen, 15596026) or RNAiso Plus (Takara Bio, 9109) was used to lyse and homogenise the cells prior to total RNA extraction. RNA was extracted either manually using the phenol-chloroform phase separation method ([Rio et al., 2010](#)) or using an RNA extraction kit (RNeasy Micro kit; Qiagen, 74004) following the kit's suggested protocol. The concentration and purity of the isolated RNA were checked using the NanoDrop spectrophotometer. RNA integrity was validated using the 18S rRNA and 28S rRNA bands observed from a 1.2% agarose gel electrophoresis run using DEPC-treated distilled water. Complementary DNA (cDNA) was synthesised from 1 $\mu\text{g}/\text{ml}$ total RNA using either the Verso cDNA synthesis kit (Thermo-Scientific, AB1453A) or the PrimeScript RT reagent kit (Takara Bio, RR037A) following the kits' prescribed protocols.

2.5 Real-time quantitative PCR (RT-qPCR)

2.5.1 Run set-up: RT-qPCR was performed using the BioRad-CFX96 Touch instrument. 5 μl reaction mixtures were set up containing the cDNA template, SYBR Green-I master mix (SYBR Fast; Kapa Biosystems, KK4600) and 10 μM each of the forward and reverse primers for the required target genes (Table 1). Glyceraldehyde-3-phosphate dehydrogenase (GAPDH) and beta-actin (ACTB) genes were selected as appropriate internal controls after screening across 5 known mammalian housekeeping genes.

2.5.2 Data analysis: Relative fold-change of mRNA expression was calculated by double normalisation of the threshold cycle (Ct) values of the treated samples against the internal control and untreated samples ([Livak and Schmittgen, 2001](#)).

2.5.3 Statistics: Analysis for the significance of results for each experiment was performed on the GraphPad Prism software version 8.4.3 using the unpaired two-tailed Multiple Student t-tests (Holm-Sidak method, with $\alpha = 0.05$) assuming normality and unequal variance in the population distributions of the sample data from the different replicates. Significance in observations for the treated samples over control samples was mentioned based on the adjusted P-values for the grouped measurements (* for $P < 0.05$, ** for $P < 0.01$, *** for $P < 0.001$, **** for $P < 0.0001$).

Table 1: List of primers used for RT-qPCR

Serial No.	Gene Name	Primer sequence
1	<i>GAPDH</i>	F: 5'-CGAGATCCCTCCAAAATCAAA-3' R: 5'-GCAGAGATGATGACCCTTTTG-3'
2	<i>ACTB</i>	F: 5'-GTCTTCCCCTCCATCGTG-3' R: 5'-TGCCAGATTTTCTCCATGTCG-3'
3	<i>B2M</i>	F: 5'-AGCTGTGCTCGCGCTACTCT-3' R: 5'-CTGAATCTTTGGAGTACGCTG-3'
4	<i>TUBB</i>	F: 5'-CTCAGGTCCTTTTGGCCAGAT-3' R: 5'-CTGCCCCAGACTGACCAAATA-3'
5	<i>18SrRNA</i>	F: 5'-CGCCGCTAGAGGTGAAATTCT-3' R: 5'-CGAACCTCCGACTTTCGTTCT-3'
6	<i>POU5F1</i>	F: 5'-AGCAAAACCCGGAGGAGT-3' R: 5'-CCACATCGGCCTGTGTATATC-3'
7	<i>SOX2</i>	F: 5'-AGACGCTCATGAAGAAGGATAAAGT-3' R: 5'-CTGCGAGTAGGACATGCTGTAG-3'
8	<i>NANOG</i>	F: 5'-GAAATCTAAGAGGTGGCAGAAAAA-3' R: 5'-GCAGAGATTCCTCTCCACAGTTAT
9	<i>PAX6</i>	F: 5'-GGCACACACACATTAACACACTT-3' R: 5'-GGTGTGTGAGAGCAATTCTAG-3'
10	<i>LMNA</i>	F: 5'-CCGCAAGACCCTTGACTCA-3' R: 5'-TGGTATTGCGCGCTTTCAG-3'
11	<i>LMNB1</i>	F: 5'-CGACCAGCTGCTCCTCAACT-3' R: 5'-CTTGATCTGGGCGCCATTA-3'
12	<i>LMNB2</i>	F: 5'-TGCGTGAGAATGAGAATGGG-3' R: 5'-ATAGTTTTTCAGTGGCTCTGGG-3'
13	<i>LBR</i>	F: 5'-CACAGTATAGCCTTCGTCCAA-3' R: 5'-CAACAGGAAGAGGAACACAGG-3'
14	<i>EMD</i>	F: 5'-CAGAGCAAGGGCTACAATGA-3'

		R: 5'-CGTCAGCATCTGGGAATGAA-3'
15	<i>NUP93</i>	F: 5'-AGAAGACGCCCTTGACTTTAC-3' R: 5'-GATATAAATTTGCCGCGCATAGG-3'
16	<i>NUP188</i>	F: 5'-CTGGGCAATCAGCAGGATATAA-3' R: 5'-AATGATCCCAAGGCCAGAAG-3'
17	<i>NUP205</i>	F: 5'-GACCCTAGAACTCAGTCCAGA-3' R: 5'-CTGTGACACCAGCGTAAGAA-3'
18	<i>NUP98</i>	F: 5'-GCTGTTGGTTCGACCCTGTT-3' R: 5'-AACAGGGTCGAACCAACAGC-3'
19	<i>LEMD3</i>	F: 5'-TTGGCCCTGAGGAAGAATTG-3' R: 5'-ACCATCACTACACCTAAGCATAA-3'
20	<i>SUN1</i>	F: 5'-CGAGGCAGTTCCAGCTATTC-3' R: 5'-GGACATCCGTGGAGAATCAAA-3'
21	<i>SUN2</i>	F: 5'-AGTCCTCTCAGGACCTTGAA-3' R: 5'-ACCAGCGACTCACTGTAGTA-3'
22	<i>SYNE1</i>	F: 5'-CTGGCAAGCAGACTGGAATA-3' R: 5'-CGGTCGAATGGCATGAATAAC-3'
23	<i>SYNE2</i>	F: 5'-CATTGCAAGCTGAACAGGAAG-3' R: 5'-CGGATATAACTGAGGGAGAAGTG-3'
24	<i>NPM1</i>	F: 5'-AAGCAGAGGCAATGAATTACG-3' R: 5'-GGAAACCGTTGGCTGTACAGA-3'
25	<i>NCL</i>	F: 5'-TGGTTTGAAAGTCTTTGGCAA-3' R: 5'-CGCATCTCGCTCTTTCTTACT-3'
26	<i>TP53</i>	F: 5'-AACGGTACTCCGCCACC-3' R: 5'-CGTGTCAACGTCGTGGA-3'
27	<i>SIRT6</i>	F: 5'-GCCAATGTAAGACGCAGTA-3' R: 5'-TCTAGGATGGTGTCCCTCAG-3'
28	<i>CTCF</i>	F: 5'-CGTTACTGTGATGCTGTGTTTC-3' R: 5'-TCATGTGCCTCTCCTGTCTA-3'
29	<i>KPNA7</i>	F: 5'-CCACCCTGCCGATCACAT-3' R: 5'-TTCGGCACAGATTCGACAAG-3'
30	<i>RXRG</i>	F: 5'-AGCTGGACTCTGGATCGTCT-3' R: 5'-ACCACATTTAGGCGAGAACCA-3'
31	<i>BANF1</i>	F: 5'-GTTCTAGTGGCTTGAGGTATC-3' R: 5'-TTCTTGCCCAGGACTTCAC-3'

32	<i>BMI1</i>	F: 5'-CCAAGTTCACAAGACCAGAC-3' R: 5'-CTTCATCTGCAACCTCTCC-3'
33	<i>BCL2</i>	F: 5'-GTGGATGACTGAGTACCTGAA-3' R: 5'-GCCAGGAGAAATCAAACAGAG-3'
34	<i>RUNX2</i>	F: 5'-GCAAGGTTCAACGATCTGAG-3' R: 5'-GGGGTCAGAGAACAACTAG-3'
35	<i>TWIST1</i>	F: 5'-GCGCTGGGGAAGATCATC-3' R: 5'-GGTCTGAATCTTGCTCAGCTT-3'
36	<i>CDH1</i>	F: 5'-CCAGTGAACAACGATGGCATT-3' R: 5'-TGCTGCTTGGCCTCAAAAT-3'

2.6 Immunofluorescence assay (IFA)

Cells were seeded onto either 18x18 mm or 22x22 mm coverslips at a density of ~0.2-0.4 million cells placed in regular cell culture dishes and plates and incubated overnight at 37°C with 5% CO₂. The cells were then washed with 1X PBS and fixed with 4% paraformaldehyde (PFA) for 10 minutes at room temperature. The fixed cells on the coverslips were then permeabilised using 0.5% Triton X-100 for 10 minutes at room temperature, followed by blocking using 1% bovine serum albumin (BSA) for 30 minutes at room temperature with intermittent washing between the steps using 1X PBS twice. Primary antibodies against the required protein targets (Table 2) were allowed to bind for 2 hours at room temperature, followed by washing with 1X PBST (0.1% Triton X-100 diluted in 1X PBS) thrice. Staining was performed using the secondary antibodies Alexa fluor- 488, 568 and 647 for 1 hour at room temperature and away from direct light, followed by three washes in 1X PBST. Counter-staining was performed using DAPI and Phalloidin. The coverslips were then washed with 1X PBS and mounted onto clean glass slides using an antifade solution and sealed.

Table 2: List of primary antibodies used for IFA

Serial No.	Protein target	Generated in	Catalogue ID	Dilution (in 1X PBST)
1	Lamin A	Rabbit	Abcam: ab26300	1:500
2	Lamin A	Mouse	Abcam: ab8980	1:500
3	Lamin A/C	Rabbit	Abcam: ab108595	1:500
4	Lamin B1	Rabbit	Abcam: ab16048	1:500
5	Lamin B1	Mouse	Abcam: ab8982	1:500
6	Lamin B2	Rabbit	Sigma: AV46356	1:500
7	Lamin B2	Mouse	Abcam: ab8983	1:500
8	NUP205	Rabbit	Novus Biologicals: NBP1-91247PEP	1:500
9	POU5F1	Mouse	DHSB: PCRP-POU5F1-1D2	1:50

2.7 siRNA-mediated gene knock-down

RNA-interference technique was implemented to transiently knock-down the gene expression of the target mRNA using small-interfering RNA (siRNA). siRNA oligonucleotides (Table 3) were purchased from Dharmacon, USA. Lyophilised siRNA nucleotides were appropriately reconstituted in 1X siRNA resuspension buffer (Dharmacon, B0020000) to make 10 mM stocks. ~0.2 million cells were seeded overnight in one well of a 6-well culture plate or a 35 mm culture dish. Transfection of each siRNA was performed using the transfection agent Lipofectamine RNAiMAX (Invitrogen, 13778150) in a reduced serum medium of Opti-MEM (Gibco, 31985) using optimised concentrations of siRNA required for 2 ml of total medium (Table 3). For transfection of each siRNA, the required volume of siRNA was added to OptiMEM in a tube, making up the volume to 250 µl and similarly, an equal volume of RNAiMAX was added to OptiMEM in a separate tube to obtain 250 µl of the mixture. The pair of tubes were mixed well, briefly vortexed and spun down before incubating for 5 minutes at room temperature. Following that, the RNAiMAX mixture was added to the siRNA mixture. This final mixture was mixed well, briefly vortexed, spun down and incubated for 30 minutes at room temperature, following which, this mixture was added to cultures containing 1.5 ml medium. An equal concentration of siRNA against the bacterial-specific gene LacZ was used as a negative control. Fresh culture medium was replenished 24 hours post-transfection. The cells were harvested 72 hours post-transfection and appropriately processed for downstream analyses. For differentiation experiments, a pulse of siRNA transfection was provided every 72 hours.

Table 3: List of siRNA oligonucleotides used for transfection

Serial No.	Gene Target	Working concentration	siRNA sequence
1	<i>LMNA</i> (oligo-2)	10 nM	5'CAGUCUGCUGAGAGGAACA-3'
2	<i>LMNB1</i> (oligo-4)	25 nM	5'-AGACAAAGAGAGAGAGAUG-3'
3	<i>LMNB1</i> (oligo-6)	25 nM	5'-AAGCUGCAGAU CGAGCUGGGC-3'
4	<i>LMNB2</i> (oligo-1)	25 nM	5'-GAGCAGGAGAUGACGGAGA-3'
5	<i>NUP205</i> (oligo-2)	25 nM	5'-AGAUGGUGAAGGAGGAUAUU-3'
6	<i>LacZ</i>	(same as target)	5'-CGUACGCGGAUACUUCGA-3'

2.8 Western blotting

Adherent cells on culture plates were washed with 1X PBS and were scraped off using cell scrapers in the Radio Immunoprecipitation Assay (RIPA) protein extraction buffer (~75 µl per 35 mm culture dish) supplemented with 1X PIC (protease inhibitor cocktail). This extract was then placed in ice and sonicated at a pulse of 3 seconds with 2 seconds rest for 30-45 seconds at an amplitude of 40-60% to generate a homogenised whole cell lysate. The lysate was then centrifuged at 13,000 rpm for 15 minutes at 4°C. The supernatant was collected in a fresh vial, processed immediately for protein estimation, or flash-frozen using liquid nitrogen and stored at -80°C. The amount of each protein lysate was estimated in duplicates using the BCA Protein Assay kit (Pierce, 23225) using bovine serum albumin (BSA; Sigma-Aldrich, A2153) standards and RIPA as blank. Readings for the test and control samples were taken at 562 nm using the Varioskan LUX or the PerkinElmer EnSight multimode microplate readers. Samples for the SDS-PAGE were prepared in 4X Laemmli buffer using 20 µg protein lysate. The resolved protein bands were transferred from the gel to a polyvinylidene fluoride (PVDF) membrane or a nitrocellulose membrane using the Dune carbonate buffer or the Towbin's buffer. The membrane was blocked using 5% skimmed milk in 1X TBST (0.1% Tween-20 in Tris buffer saline) for 1 hour at room temperature before incubation with primary antibodies (diluted as shown in Table 4) overnight at 4°C. GAPDH was used as the internal loading control. The membrane was then incubated with HRP-tagged secondary antibodies against Mouse and Rabbit (diluted 1:10,000 in 5% skimmed milk in 1X TBST). The blots were developed using the Clarity chemiluminescence detection kit (Bio-Rad, 1705061). Images were acquired using the ImageQuant Las 4000 instrument at incremented 10 seconds of exposure until saturation of the bands. Fold-change expression change in the target protein levels of treated samples relative to control samples was quantified on the Fiji image analysis software after normalisation of the band area of target protein blots over the internal control protein (GAPDH) blots.

Table 4: List of primary antibodies used for Western blotting

Serial No.	Protein target	Generated in	Catalog ID	Dilution (in 1X TBST)
1	Lamin A	Rabbit	Abcam: ab26300	1:1,000
2	Lamin A/C	Rabbit	Abcam: ab108595	1:1,000
3	Lamin B1	Rabbit	Abcam: ab16048	1:500
4	Lamin B2	Mouse	Abcam: ab8983	1:500
5	NUP93	Rabbit	Abcam: ab168805	1:500
6	NUP188	Rabbit	Abcam: ab86601	1:1,000
7	NUP205	Rabbit	ATLAS: HPA024574	1:500
8	POU5F1	Mouse	DHSB: PCRP-POU5F1-1D2	1:500
9	SOX2	Mouse	DHSB: PCRP-SOX2-1B3	1:500
10	NANOG	Mouse	DHSB: PCRP-NANOGP1-2D8	1:500
11	GAPDH	Rabbit	Sigma: G9545	1:5,000

2.9 Microscopic imaging

2.9.1 Image capture: Bright-field images were periodically captured during the progression of knock-down and differentiation of the NT2/D1 using the Zeiss Axio Vert.A1 microscope at 10X and 20X magnifications in order to observe growth patterns of the cell cultures and note morphological changes in the cell shape. Fluorescently-labelled cells and nuclei were imaged over the 63X Plan-Apo1.4 NA oil-immersion objective lens using the Zeiss LSM-710 confocal microscope and Zeiss LSM-780 multiphoton microscope using the appropriate excitation laser filters (DAPI- 405 nm, Alexa-Fluor Green- 488 nm, Alexa-Fluor Red- 568 nm, Alexa-Fluor Far-red- 647 nm) at 0.6X and 2X digital zoom for image quantification and representation respectively. The line averaging was set to 4.0 with a scan speed of 9.0. Z-stacks of the labelled samples were obtained for 3-dimensional quantification.

2.9.2 Image analyses: The images were analysed using the Fiji image analysis software (Schindelin et al., 2012). Phalloidin and DAPI boundaries were used for quantifying cell and nuclear shapes respectively. Quantitative protein estimation for inner-nuclear proteins was performed by quantifying the mean grey values (if uniform staining) or integrated density values (if non-uniform staining) for the stain within the nuclear boundary. Quantification for lamins was performed differentially for localisation in the nuclear envelope and in the nucleoplasm using an automated algorithm developed in the lab (summarised in Fig. 2 and provided for use in extended methods section 8.1). Statistical analyses for the significance of results were performed on the GraphPad Prism software version 8.4 using the unpaired two-tailed Multiple Student t-test assuming normality and equal variance in the population measurements.

Figure 2

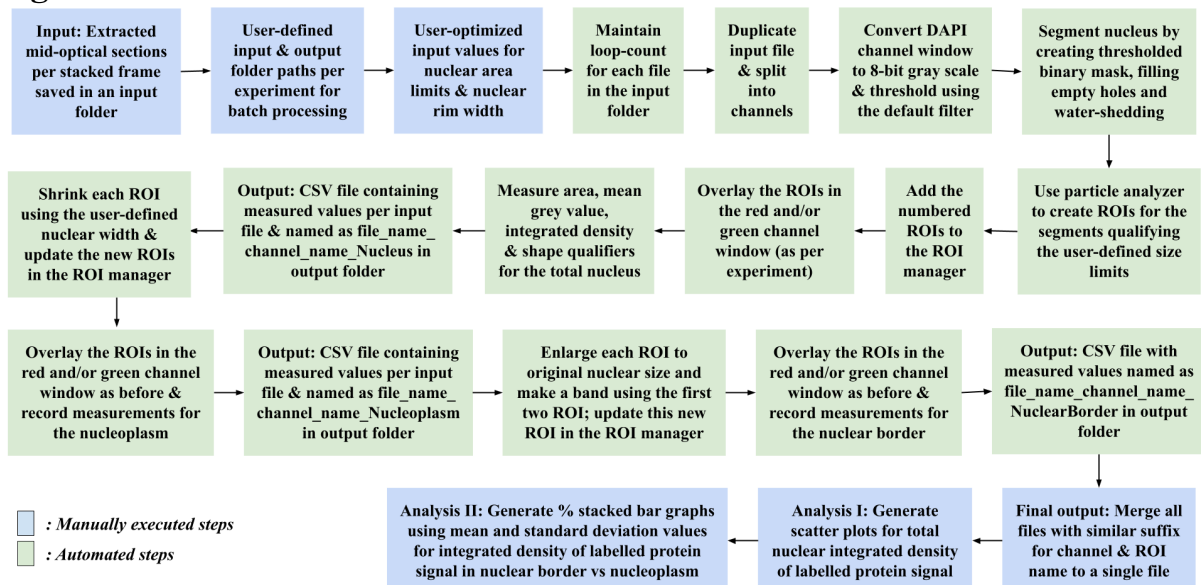


Fig. 2: Schematic workflow of lamin quantification from immunofluorescence assays. The represented workflow describes the automated batch-processing of measurements for signal densities, and area and shape-descriptors across all nuclei in a frame and over multiple frames of pre-extracted mid-optical sections obtained from the raw 3-dimensional hyper-stack files.

2.10 3'mRNA sequencing

A single-ended transcriptome sequencing was performed using one fragment per gene from the 3' end to count and analyse the global differential gene expression between the treated and control samples using a multi-step process (summarised in Fig. 3).

2.10.1 RNA concentration and quality validation: Total RNA for the required samples was extracted from TRIzol-lysed cells using RNA isolation and purification columns (Qiagen, 74004). The concentration of the extracted RNA was measured by a fluorimetric analysis using the Qubit RNA High Sensitivity Assay kit (Invitrogen, Q32852), and the readings were taken using a Qubit 4.0 fluorometer. The integrity of the RNA samples was checked on a chip-based electrophoresis unit using the Agilent RNA Nano 6000 kit (Agilent Technologies, 5067-1511). The loaded chips were then run on the Agilent 2100 Bioanalyzer instrument. Samples were processed for further steps provided an RNA integrity number (RIN) of 6.5 or above was obtained. Alternately, samples were run for a 1.2% RNA agarose gel electrophoresis and checked for clear 18S and 28S rRNA bands.

2.10.2 Library preparation: The validated RNA samples were processed for a multi-step cDNA library preparation protocol using the QuantSeq 3'mRNA FWD library preparation kit (Lexogen, 139) as recommended in the kit manual. The prepared libraries were subjected to magnetic bead-based purification using the QuantSeq kit in order to obtain average library sizes in the range of ~400-800 base pairs.

2.10.3 Library amplification: To estimate the optimal number of amplification cycles for the libraries, an RT-qPCR was performed on the purified libraries using 2.5X SYBR Green-I dye (Sigma-Aldrich, S9430) diluted in DMSO, enzyme and primers from the QuantSeq PCR add-on kit (Lexogen, 020.96) as recommended. The cycle number corresponding to 50% of the maximum fluorescence was noted. Then, each library was ligated to unique molecular identifiers (UMI; Lexogen, 139) containing the 6-nucleotide adapters and sequencing primers to facilitate multiplexed sequencing by barcoded indexing of individual samples. These indexed libraries were then amplified by an end-point PCR using three fewer cycle numbers than estimated by the RT-qPCR to prevent over-amplification of the samples. The amplified libraries were again purified using magnetic beads to remove adapter-adapter linker contaminants and over-amplified artefacts.

2.10.4 Library concentration and quality check: The concentration of the purified final libraries was observed on the Qubit 4.0 fluorometer using the Qubit dsDNA High Sensitivity Assay kit (Invitrogen, Q32851). The quality of the library was checked by employing a chip-based electrophoresis technique using the Agilent DNA High Sensitivity kit and running it on the Agilent 2100 Bioanalyzer instrument. The average library size was noted per sample. Samples were processed further if the library distribution was between 150-1000 base pairs and devoid of lower or higher molecular weight contaminants.

2.10.5 Library molarity calculation: The molarity of the individual libraries was calculated as suggested by the QuantSeq kit manual:

Molarity = [Library concentration (ng/μl) x 10⁶] / (660 x average library fragment size (base pairs))

2.10.6 Pre-sequencing sample preparation: The NextSeq 500/550 Mid-output 150 cycles v2.5 kit (Illumina, 20024904) was used for preparing the sample libraries and the spiked internal control library PhiX (Illumina, FC-110-3002) for the sequencing run. The libraries were diluted to 2 nM and pooled together in equal volumes of 10 μl, ensuring a final mixture concentration of 2 nM as recommended by the kit manual. The concentration of this mixture was cross-validated using a Qubit DNA analysis. The sample library mixture and the PhiX library were then prepared for loading, ensuring ~5 million reads per sample:

- **Denaturation:** 10 μl of the pooled library mixture was added to 10 μl of 0.2 N freshly prepared NaOH, vortexed briefly, centrifuged at 280 × g for 1 minute and then incubated at room temperature for 5 minutes. Then, 10 μl of freshly-prepared 200 mM Tris-HCl (pH 7) was added to the mixture, vortexed briefly and then centrifuged at 280 × g for 1 minute. The same procedure was followed for PhiX separately.
- **Dilution:** The denatured library pool was diluted to 20 pM using 970 μl prechilled HT1 hybridisation buffer and then vortexed briefly, followed by centrifugation at 280 × g for 1 minute. This mixture was then further diluted to a loading concentration of 1.35 pM to get a total volume of 1.3 ml, followed by invert-mixing of the sample tube and pulse centrifuging. The same procedure was followed for PhiX separately.

2.10.7 Sequencing run: The reagent cartridge was thawed in distilled water at room temperature 1 hour prior to sequencing, and the flow cell cartridge was equilibrated at room temperature 30 minutes prior to sequencing. The final loading mixture was prepared by adding 13 μl of the PhiX library to 1287 μl of the pooled sample library mixture to give 1% PhiX in a total volume of 1.3 ml with a 1.35 pM concentration. The final mixture was then loaded onto the reagent cartridge, and all the cartridges were loaded onto the prescribed locations in the Illumina NextSeq 550 instrument system. After entering the information relevant for a single-ended RNA sequencing run on the sequencer software, the run was started.

2.11 Sequencing data analysis

2.11.1 File generation: The raw files were obtained in the form of binary base call peak (.bcl) files. These files were then converted into compressed .fastq files using the Linux command based-tool bcl2fastq provided as a stand-alone application by Illumina using a sample sheet containing adapter sequences as input. The fastq.gz files obtained for the four different flow cell lanes were merged into a single fastq.gz file per sample using the 'cat' command-based concatenation function.

2.11.2 File quality control, alignment & mapping, read count: The merged fastq.gz files were then processed for the Quantseq 2.3.6 FWD pipeline provided by the BlueBee genomics data analysis software (summarised in Fig. 3). This included evaluating the quality of the sample reads, and trimming the adapters and low-quality reads. The trimmed reads were then

mapped and annotated to their respective gene locations by aligning them against the reference human genome sequence (GRCh38). Read count tables were then generated per gene represented in the sample.

2.11.3 Differential gene expression analysis: The processed sample files were subjected to a differential gene expression analysis based on the read counts per gene using the Quantseq DE 1.4.0 pipeline provided by BlueBee (Fig. 4). The output tables were used to generate principal component analyses (PCA) between all the analyzed samples for a group to show clusters based on similarity in gene expression levels. Possible outlier samples were removed from downstream analyses after analysing the PCA clustering and then heatmaps for significantly upregulated and downregulated genes between the treated and control samples were generated.

Figure 3

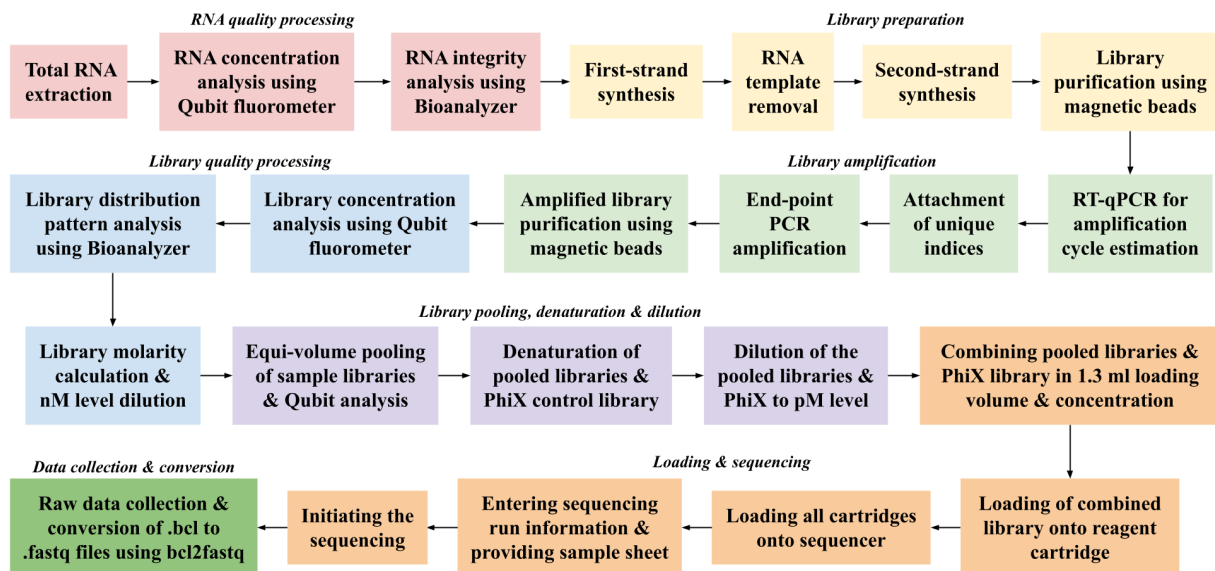


Fig. 3: Schematic pipeline for 3'mRNA sequencing. The multi-step protocol for sample preparation and validation, running the sequencer and collecting the data has been summarized in this schematic.

Figure 4

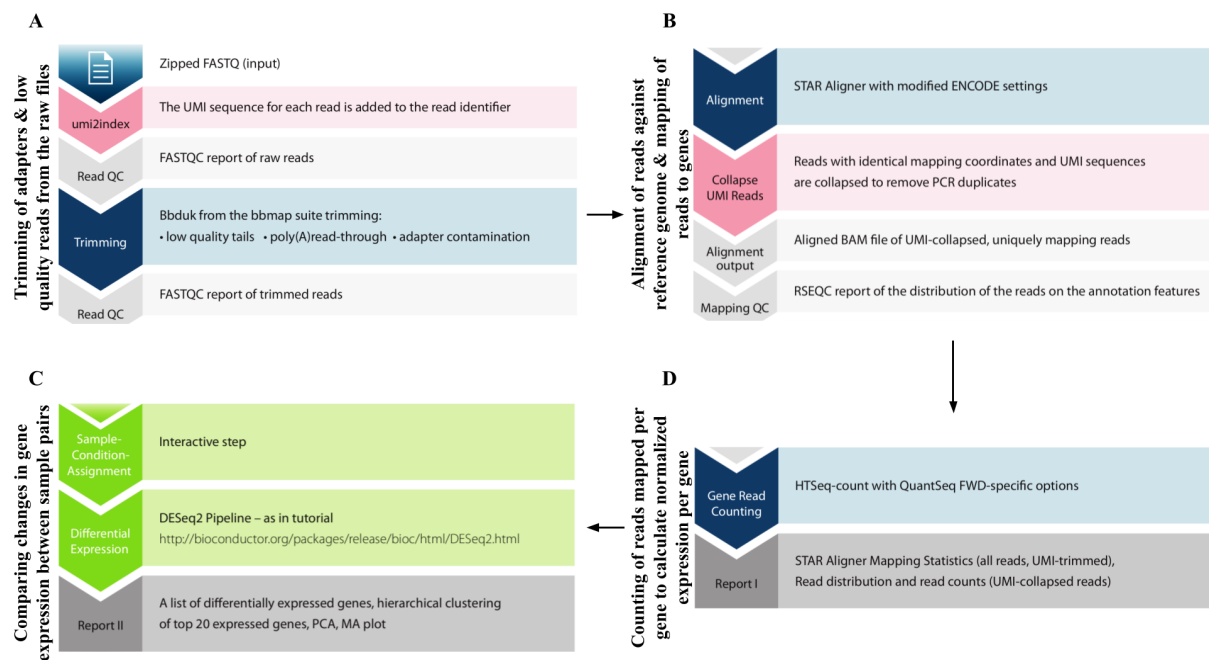


Fig. 4: Workflow of differential gene expression analysis using BlueBee genomics analysis server. The different interactive BlueBee modules and their working principles have been briefly summarized to illustrate the step-wise analysis of the sequencing output files. (Image has been modified from <https://www.lexogen.com/lexogen-data-analysis-solutions-on-bluebee-platform/>).

2.12 Network analysis

The different data sets for the network analysis were derived from literature and protein-protein interaction studies were performed using the enrichment parameter of the STRING tool version 10.5 and the networks were visualized using Cytoscape 3.9.1.

3. Results

3.1 NT2/D1 is a differentiable cell system

NT2/D1 cells were first validated by karyotyping, which was performed by counting the number of chromosomes visible in a metaphase-arrested state of the cells across the population ($n=52$) (Fig. E1A). A majority of cells in the studied population ($\sim 54\%$) showed a chromosome number of 60-62, which is similar to the ATCC-accepted modal chromosome number of 62-63 in NT2/D1 (Fig. E1B-C). Karyotyping for a higher sample size of cells performed in more biological replicates is likely to add more confidence to the conclusion drawn. The NT2/D1 cells, when subjected to a pre-optimized differentiation pipeline (Fig. 5A), exhibited gradual morphological changes upon pulsed RA treatment for 8-10 days. These changes were observed in the form of elongation, flattening and branching of the cells (Fig. 5B), as quantified by the increase in the cell area (Fig. 5C) and decrease in the circularity of the cell boundary as the cells become more angular with projections during differentiation (Fig. 5D). These observations are characteristic of neuronal cells (Wilson et

al., 2018), indicating that the undifferentiated NT2/D1 cells are likely to have differentiated into neuronal cells upon RA treatment. Upon performing qRT-PCR analysis on the RA-treated cells compared to the control cells treated with the RA-diluent DMSO, the levels of pluripotency markers like *POU5F1* (also known as *OCT4*), *SOX2* and *NANOG* were observed to have significantly downregulated (Fig. 5E) while the transcript levels of the neuronal development marker *PAX6* were significantly upregulated (Fig. 5F), thus validating loss of pluripotency and successful progression of differentiation of the NT2/D1 cells into the neuronal lineage. Further, the levels of nuclear lamin subtypes also changed upon differentiation (Fig. 5G) as seen from the changes in their transcript levels post 8 days of differentiation. It was observed that the *LMNA* levels were highly upregulated (4-folds) upon RA treatment followed by a relatively less upregulation in *LMNB2* levels (2-folds), while the levels of *LMNB1* and the lamin-associated nuclear envelope protein *LBR* showed no considerable change. However, wide variability in the expression levels of lamins was seen across the two biological replicates, especially in the case of *LMNA*. Analyses of the gene expression levels from more independent biological replicates are likely to strengthen our preliminary conclusions with a statistical significance. Since lamins are a major component of the nuclear envelope, changes in their expression levels are indicative of possible rearrangement in the nuclear membrane structure and function during differentiation. This makes the NT2/D1 cell line an appropriate differentiable model for studying the role of nuclear lamins and other nuclear envelope proteins during cellular differentiation (Fig. E2A).

Figure 5

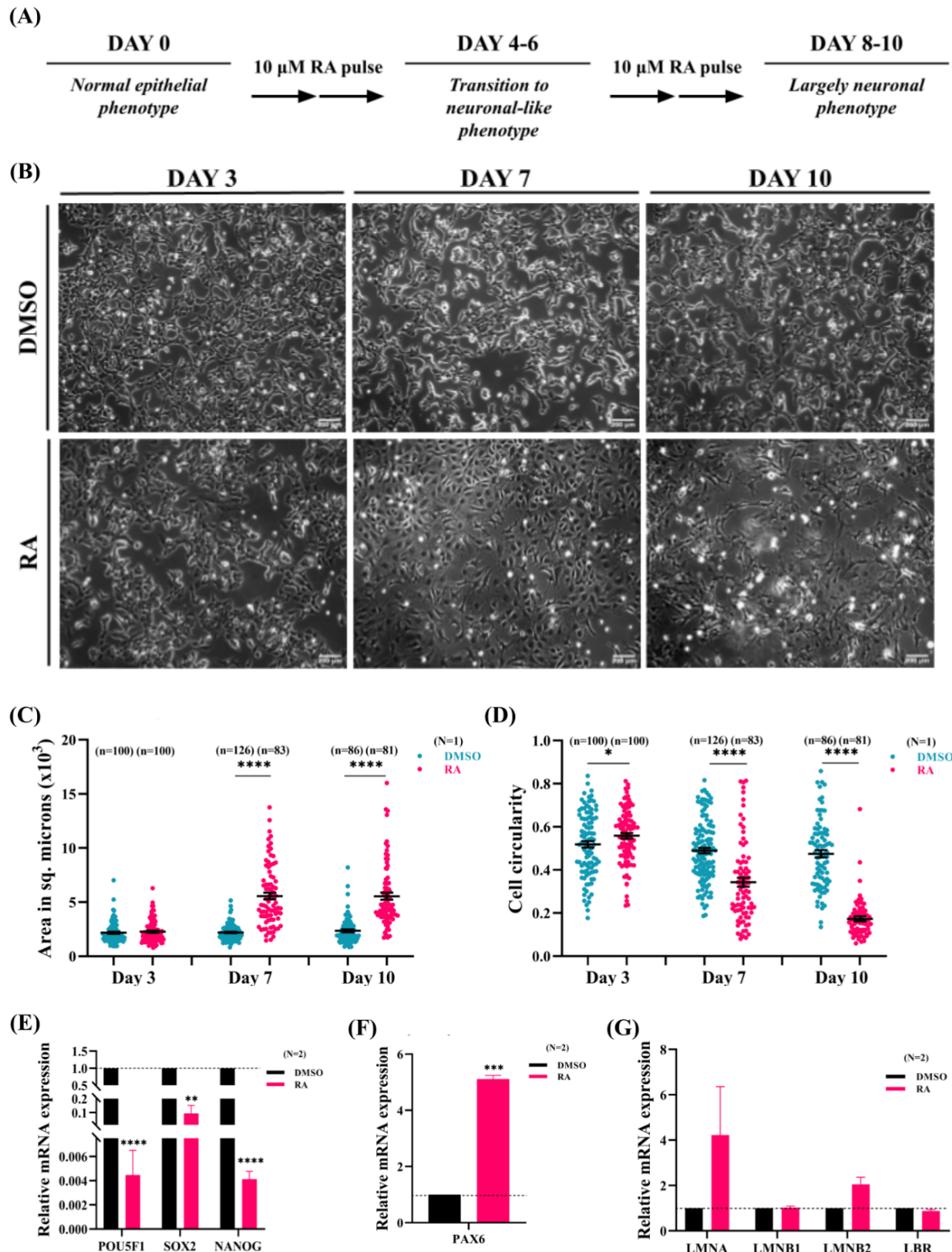


Fig. 5: NT2/D1 cells differentiate into neuronal cells upon RA treatment. (A) Schematic depicting one complete course of daily-pulsated RA treatment used for differentiation of the NT2/D1 cells over 8-10 days, starting with the first dose on Day 0. (B) Bright-field images showing morphological changes in the cell during the progression of RA treatment from a largely undifferentiated state on Day 3 to a partially differentiated population of cells on Day 7 to a majorly differentiated population of cells by Day 10 of RA treatment. (Scale bar=200 μ m). (C) Cell area increases upon consistent RA treatment as quantified from the bright field images.

(N=1, n=~80-130, as shown in plot). **(D)** Circularity index for the cell shape gradually decreases during differentiation as quantified from the bright field images. (N=1, n=~80-130, as shown in plot). **(E-F)** Transcript levels of the (E) pluripotency markers *POU5F1*, *SOX2* and *NANOG* decrease while the (F) neuronal differentiation-specific marker *PAX6* increases by 8 days of differentiation. (N=2, n=6). **(G)** Transcript levels of nuclear lamins are affected upon 8 days of differentiation. (N=2, n=6). Error bars represent the standard error of the mean.

3.2 Neuronal differentiation in NT2/D1 cells affects the expression of lamins

The different lamin subtypes Lamins A, B1 and B2 were labelled using the immunofluorescence technique with red, yellow and green stains respectively, in partially differentiated (6 days RA treatment) and differentiated (10 days RA treatment) NT2/D1 cells (Fig. 6A) to quantify single-cell level protein expression levels of nuclear lamins during the progression of differentiation. The nuclear area consistently increased with the progression of differentiation in RA-treated cells compared to control cells (Fig. 6B), indicating an expansion in the nucleus along with cellular expansion (as shown in Fig. 5C). The expression levels of the proteins were calculated using the integrated density of the signal emitted by the labelled proteins in the RA-treated cells as compared to the control DMSO-treated cells. Although Lamin A levels were decreased compared to control upon 6 days of RA treatment, their levels were significantly upregulated upon 10 days of continued RA treatment (Fig. 6C). Lamin B1, though upregulated post 6-days of RA treatment, showed an upregulation in expression between Day 6 and Day 10 of RA treatment. On the other hand, B2 levels were consistently overexpressed over the course of RA treatment (Fig. 6C). This indicates that upregulation in the B-type lamins is associated with the initiation as well as the progression of differentiation, whereas upregulation in Lamin A is associated with the later stages of differentiation. This observation is consistent with the earlier observation for the upregulated transcript levels of Lamin A after 8 days of differentiation (as shown in Fig. 1G).

The differential localisation of the lamin subtypes in the nuclear border and nucleoplasm was quantified using the density of emitted signals in either nuclear fraction. Lamin A and B2 did not show considerable changes in their localisation between the 6-day and 10-day RA treated cells (Fig. 6D). However, Lamin B1 showed about 15% more nucleoplasmic localisation upon 10 days of RA treatment as compared to 6 days of treatment (Fig. 6D), although observations from more biological replicates are required to conclusively comment upon the relative localization differences of the lamins during differentiation.

An important observation is the stoichiometry of A-type to B-type lamins expression during changes in the cell fate. An increased Lamin A/B ratio was observed upon differentiation in the intermediate stage (day 6) as well as in the later stage of differentiation (Day 10) when compared between RA-treated and undifferentiated cells, as quantified from the average single-cell protein expression data (Fig. 6E). However, upon observing the relative Lamin A/B protein expressions between Day-6 differentiated and Day-10 differentiated cells, the ratio decreased considerably by ~2-folds (Fig. 6E). This shows that the relative expression of Lamin A is much higher compared to B-type lamins in the intermediate stage of differentiation whereas, towards the later stages of differentiation, the expression of A and B-type lamins are rather comparable, indicating the importance of co-expressivity of both lamin types. However, more replicative observations are required to conclusively comment

upon the selective importance of A-type and B-type lamins across differentiation with statistical significance at the population-level observation.

Figure 6

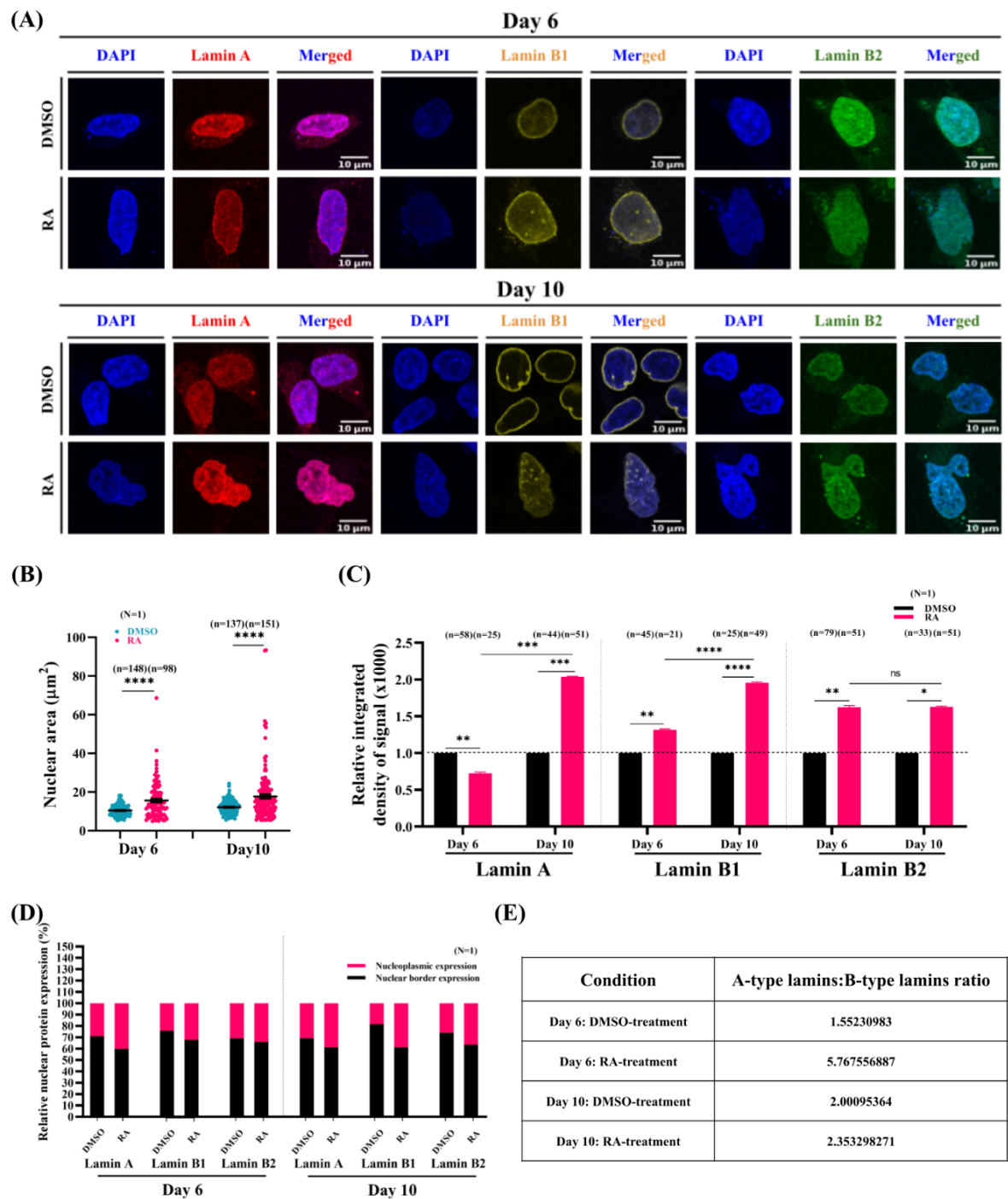


Fig. 6: Expression of nuclear lamins changes during differentiation of NT2/D1 cells. (A) Representative immunofluorescent staining of Lamin A (red), Lamin B1 (yellow) and Lamin B2 (green), counterstained by nuclear marker DAPI (blue) in 6-day and 10-day differentiated cells. (Scale bar=10 μ m). (B) Nuclear area increases over the course of differentiation. (N=1, n=~90-150, as shown in plot). (C) Single-cell protein expression of lamins A, B1 and B2 as quantified from Fig. 6A in partially differentiated cells (Day 6) and majorly differentiated cells (Day 10). (N=1, n=~20-60, as shown in plot). (D) Differential localisation of the fraction of the lamins in the nuclear border vs nucleoplasm represented as the percentage fraction of total nuclear lamin expression for Lamins A, B1 and B2 in 6-day and 10-day differentiated cells. (N=1, n=same as in Fig. 6B). (E) Stoichiometric Lamin A/B expression ratio upon differentiation in the intermediate stage (day 6) and later stage of differentiation (Day 10). Error bars represent the standard error of the mean.

3.3 Loss of lamin subtypes affects stemness and differentiability of NT2/D1 cells

The different lamin subtypes were selectively knocked-down using siRNAs targeting the *LMNA*, *LMNB1* or *LMNB2* genes in NT2/D1 cells to study the effect of their downregulated expression on the cell pluripotency and hence, its differentiability. Based on earlier optimizations in the lab by kill-curve analyses of titrated siRNA concentrations, the most effective dose with the least lethality was selected for the transfections (10 μ M siLMNA, 25 μ M siLMNB1 and 25 μ M siLMNB2). The cells were observed for a period of 72 hours, until which the transient transfection has been observed to be effective in these cells. (Benjamin et al., unpublished data). There was no perceptible difference in the morphology of the cells in terms of shape, as observed from their bright-field images (Fig. 7A). Transcript levels of the pluripotency factors *POU5F1* and *SOX2* were significantly downregulated upon depletion of all three lamin subtypes, while *NANOG* showed variability in its expression levels with upregulation upon Lamin A knock-down and downregulation upon B-type lamins knock-down (Fig. 7B-D). On the other hand, *PAX6* transcript levels were upregulated for all three lamin knock-downs, although statistical significance could not be achieved in these results due to the wide variability in the expression levels between the replicates (Fig. 7B-D). Taken together, these observations suggest that depletion of any nuclear lamin subtype is likely to decrease the pluripotency of NT2/D1 cells and might prime them to differentiate into a neuronal lineage.

Furthermore, protein-protein interaction studies were performed for each of the three lamin gene products with a data set of known pluripotency critical genes (PCGs) in humans (Ghosh and Som, 2020). The networks revealed that Lamin A is weakly associated with the *NANOG* and *ESRP1* PCGs (Fig. 7E). Similarly, Lamin B1 was found to be a weak interactor of *NANOG* (Fig. 7F). On the other hand, Lamin B2 does not associate directly with any PCGs, but it interacts with both Lamins A and B1, which in turn, interact with PCGs. Since lamins are an integral part of the nuclear envelope and associate with the other nuclear membrane proteins, an interaction network analysis was performed using the pluripotency factors and different nuclear membrane proteins (Fig. E3A).

A global transcript level differential gene expression analysis was attempted from the data obtained from the 3' mRNA sequencing results for NT2/D1 cell samples with individual Lamin A, B1 and B2 depletion, but the analysis failed to show significantly altered gene expressions due to technical errors incurred while preparing samples for the sequencing.

Figure 7

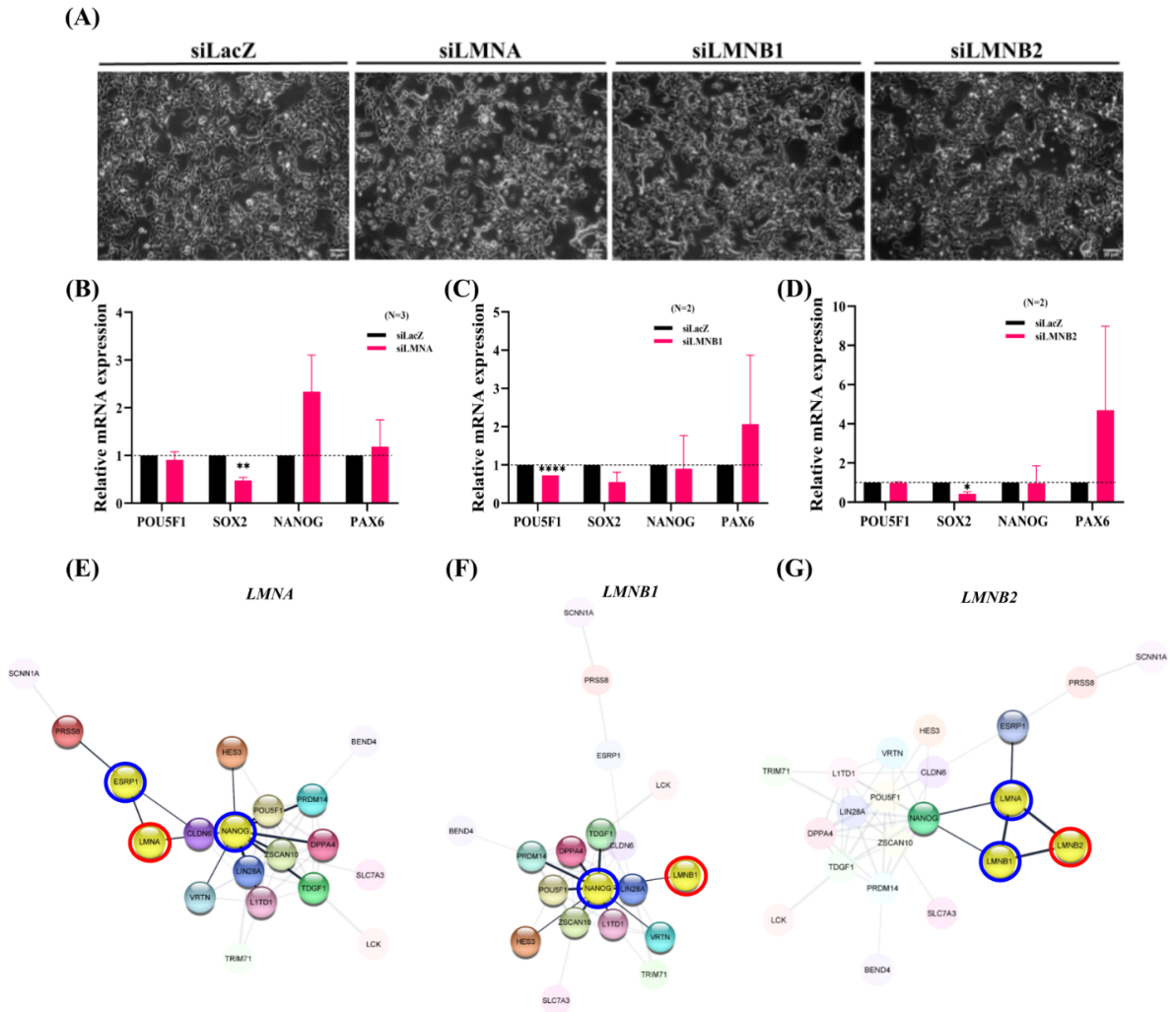


Fig. 7: Depletion of the lamin subtypes affects the pluripotency of NT2/D1 cells. (A) Bright-field images show representative changes in cell density and morphology after 72 hours of knock-down of the different lamins subtypes compared to the control (siLacZ transfected cells). (B-D) Transcript levels of pluripotency (*POU5F1*, *SOX2*, *NANOG*) and differentiation-specific marker (*PAX6*) upon knock-down of (B) Lamin A, (C) Lamin B1, and (D) Lamin B2 show considerable downregulation of *POU5F1* and *SOX2* during depletion of the lamin subtypes. (N=3, n=9). (E-G) Direct critical pluripotency interactors (blue-rimmed) of lamins (red-rimmed) and their first neighbours (highlighted without rims) are shown for (E) Lamin A, (F) Lamin B1, and (G) Lamin B2. Error bars represent the standard error of the mean.

3.4 Loss of individual lamin subtypes affects the expression of the other lamin subtypes

All the three major subtypes of lamins contribute to the proper functioning of the nuclear envelope, but also have unique regulatory roles (Patil and Sengupta, 2021). To study how each lamin subtype affects the expression of the other two subtypes, each lamin was selectively knocked-down and the transcript levels of the other lamins were studied. It was observed that upon Lamin A depletion, Lamin B1 and Lamin B2 expression levels were slightly upregulated (Fig. 8A). For Lamin B1 knock-down, Lamin A was slightly downregulated, whereas Lamin B2 was considerably upregulated (Fig. 8B). Similarly, it was

found that for Lamin B2 knock-down, Lamin A was slightly downregulated while Lamin B1 was considerably upregulated (Fig. 8C). This indicates that the expression of B-type lamins is not significantly affected by the loss of Lamin A. However, each of the B-type lamins appears to show a possible compensatory upregulation upon the depletion of the other B-type lamin, although statistical significance could not be achieved due to the wide variation in the expression levels between the replicates. On the other hand, Lamin A seems to be relatively dispensable when B-type lamins are depleted.

Additionally, protein levels of the lamins were analysed to validate the knock-down across the three lamin subtypes using the Western blotting technique. The representative images showed qualitative downregulation in protein expression of the knocked-down genes (Fig. 8D). Quantification of the relative protein levels showed that Lamin B1 had been upregulated slightly while Lamin B2 had been notably upregulated upon loss of Lamin A (Fig. 8E). On the other hand, for either of the B-type lamins loss, the other B-type lamin appeared to be considerably upregulated while Lamin A was considerably downregulated in either case. This observation largely agrees with the transcript expression levels (Fig. 8A-C).

Figure 8

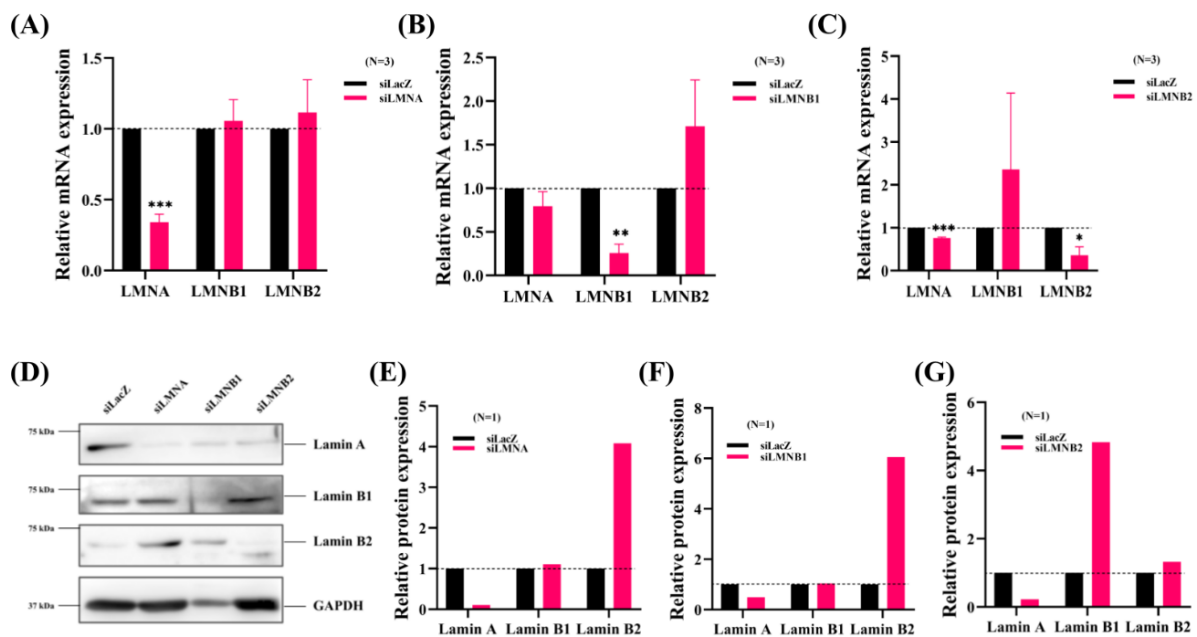


Fig. 8: Loss of different lamin subtypes affects the expression of the other lamin subtypes. (A-C) Transcript levels of the other two lamins change upon knock-down of (A) Lamin A, (B) Lamin B1 and (C) Lamin B2. (N=3, n=9). (D) Representative image for validation of Lamin A, B1 and B2 depletions using western blotting. (E-G) Fold-change of protein expressions of Lamin A, B1 and B2 in each of the knock-down conditions. (N=1, n=3). Error bars represent the standard error of the mean.

3.5 Depletion of different lamins affects differentiation of NT2/D1 cells

NT2/D1 cells with knocked-down lamins were subjected to RA treatment to study how the progression of differentiation was affected by the depletion of each of the lamin subtypes. Pulses of siRNA were transfected every 72-hours to maintain the lamins in a depleted state and the lamin-depleted cells were simultaneously administered with daily RA treatment for 8

days, beginning 24 hours post the first siRNA transfection. An IFA was performed with Lamin A and Lamin B2 labelled in red and green stains respectively to study the representative expression of A-type and B-type lamin proteins at the single-cell level after 8 days of RA treatment (Fig. 9A). It was observed that Lamin A levels were upregulated upon RA treatment of cells with depleted Lamin B1 or Lamin B2 (Fig. 9B). Similarly, Lamin B2 levels were also upregulated upon RA treatment of cells with depleted Lamin A and Lamin B1 (Fig. 9B).

Further, transcript level data was analysed using RT-qPCR for target gene groups such as lamins, pluripotency factors and differentiation marker *PAX6* (Fig. 9D-L). In the case of 8-day differentiation with loss of Lamin A, the *LMNA* levels were significantly downregulated further upon differentiation (Fig. 9D). Lamin B1 was also downregulated slightly upon Lamin A knock-down and showed further downregulated after 8-days of RA treatment (Fig. 9D). However, Lamin B2 was considerably overexpressed upon loss of Lamin A and did not show significant changes upon differentiation. As for the pluripotency levels, the levels of *POU5F1* seemed unaffected by the loss of Lamin A but was significantly downregulated upon differentiation (Fig. 9G). Interestingly, *SOX2* levels remained unchanged across all replicate data sets upon knock-down as well as differentiation (Fig. 9G). *NANOG* levels appeared to be downregulated upon knock-down of Lamin A and slightly increased with differentiation (Fig. 9G). Surprisingly, *PAX6* levels decreased upon Lamin A knock-down and further decreased upon differentiation, raising the question of whether loss of Lamin A is unfavourable for neuronal differentiation of NT2/D1 by RA treatment. (Fig. 9J).

In the case of Lamin B1 knock-down, huge variability was observed between the replicate data sets. Lamins A and B2 appeared to decrease in the siLMNB1 samples but increased upon differentiation (Fig. 9E). Lamin B1 also appeared to have recovered in its transcript levels and overexpressed upon differentiation. (Fig. 9E). Upon observing the pluripotency factors expression, *POU5F1* levels decreased upon Lamin B1 knock-down but further got downregulated with differentiation (Fig. 9H). However, *SOX2* and *NANOG* levels did not significantly change upon either knock-down or differentiation (Fig. 9H). *PAX6* levels increased upon Lamin B1 knock-down and further increased upon differentiation (Fig. 9K).

In the case of Lamin B2 knock-down, Lamin A levels could not be targeted due to a technical failure where the Ct value for the samples could not be read from the RT-qPCR plate. Lamin B1 levels were seen to get upregulated upon Lamin B2 knock-down (Fig. 9F), as was earlier observed. However, the Lamin B2 levels decreased upon differentiation. *POU5F1* and *SOX2* profiles for Lamin B2 knock-down were very similar to those with Lamin A knock-down. (Fig. 9I). *NANOG* levels did not show any significant change upon knock-down or differentiation (Fig. 9I). *PAX6* levels increased similarly for Lamin B2 knock-down as that of B1 knock-down (Fig. 9L). This observation is consistent with the earlier speculation that loss of B-type lamins promotes differentiation in NT2/D1 cells.

Figure 9

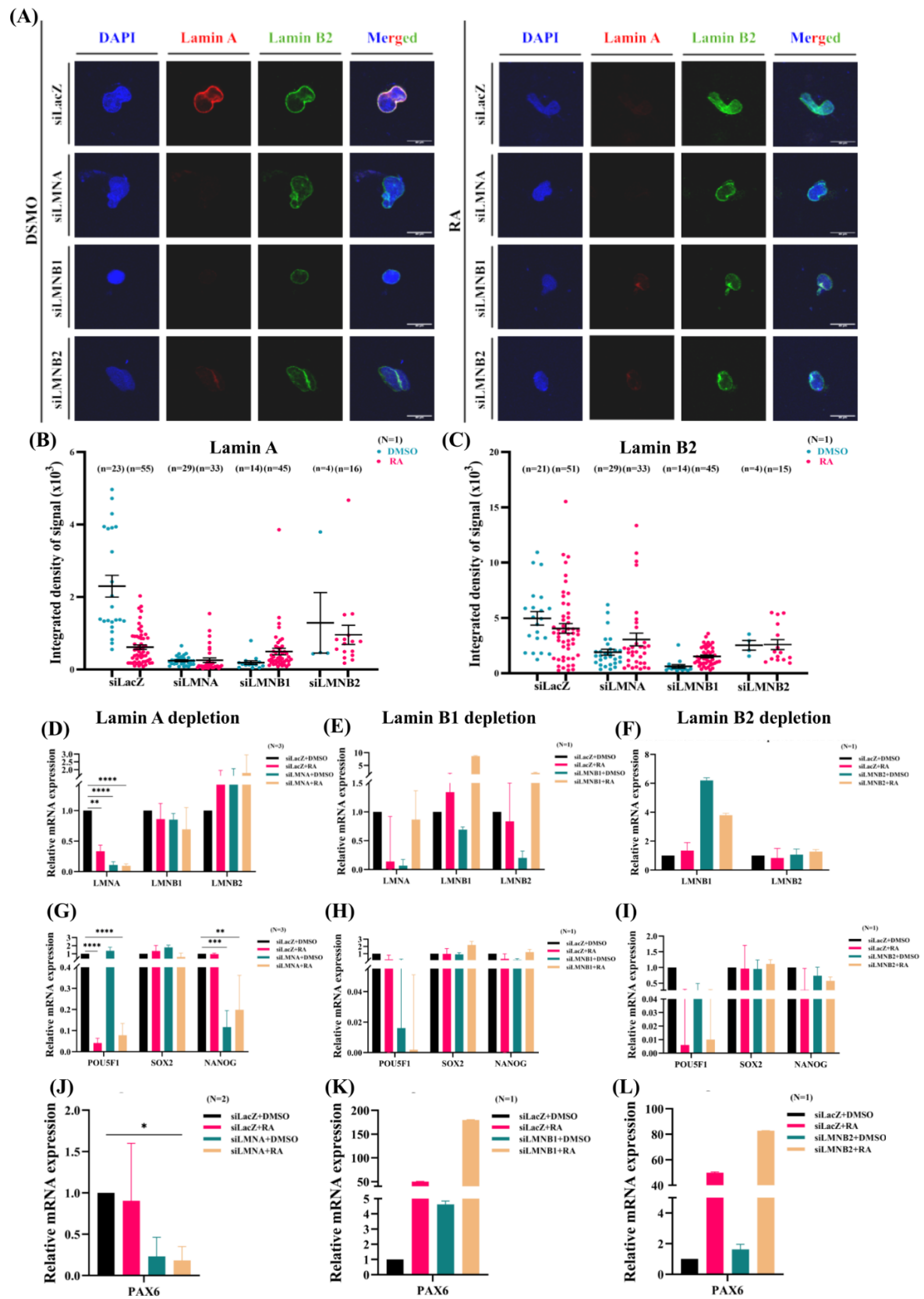


Fig. 9: RA treatment in different lamin-depleted cells affects differentiation and expression of other lamins. (A) Representative immunofluorescent staining of Lamin A (red) and Lamin B2 (green), counterstained by nuclear marker DAPI (blue) in Lamins A, B1 and B2-depleted cells. (B-C) Single cell-level protein expression data using IFA shows the change in expression of (B) Lamin A and (C) Lamin B2 proteins upon knock-down of other lamin subtypes. (N=1, n=~10-60, as shown in plot). (D-F) Transcript levels of lamin subtypes upon 8 days of differentiation in cells with (D) Lamin A (N=3, n=9), (E) Lamin B1 (N=1, n=3), and (F) Lamin B2 (N=1, n=3) knock-down. (G-I) Transcript levels of pluripotency markers upon 8 days of differentiation in cells with (G) Lamin A (N=3, n=9), (H) Lamin B1 (N=1, n=3), and (I) Lamin B2 (N=1, n=3) knock-down. (J-L) Transcript levels of differentiation-specific marker *PAX6* upon 8 days of differentiation in cells with (J) Lamin A (N=3, n=9), (K) Lamin B1 (N=1, n=3), and (L) Lamin B2 (N=1, n=3) knock-down. Error bars represent the standard error of the mean.

3.6 Lamins show possible cross-talk with nucleoporins

Subunits of the NUP-93 complex proteins were analysed at the transcript levels upon all three lamin knock-downs to check the effect of lamins loss-of-function on Nups after 72 hours of siRNA transfections against *LMNA*, *LMNB1* and *LMNB2*. The loss of Lamin A appeared to upregulate all three NUP93-complex proteins (Fig. 10A) while the loss of both B-type lamins appeared to downregulate them (Fig. 10B-C), although readings across the replicates are variable and more replicated observations are required to analyse the significance of these observations. Further, levels of all Nups decreased upon differentiation in the siLMNA-treated samples (Fig. 10D). Upon differentiation of the siLMNB1-treated samples, NUP93 and NUP188 were downregulated while NUP205 was upregulated (Fig. 10E). As for the siLMNB2-treated samples, NUP93 and NUP188 levels were not affected considerably while NUP205 was upregulated (Fig. 10F). This indicates a stronger correlation between levels of NUP205 and the B-type lamins during differentiation as compared to the other Nups of the complex.

Since Nups levels were shown to be affected by the loss of lamins, it is likely that loss of Nups might affect lamin expressions. NUP205 was considered as the candidate NUP93-subcomplex protein to observe these effects. Bright-field images of the siNUP205-transfected cells did not show significant qualitative changes in the cell morphology over the 72 hours of transfection (Fig. 10G). The efficiency of the *NUP205* knock-down was validated at the transcript level by RT-qPCR (Fig. 10H). The levels of all three lamin subtypes appeared to have been downregulated upon loss of NUP205 (Fig. 10I), and so did the levels of the pluripotency factors (Fig. 10J). This is consistent with the earlier observations indicating that loss of lamins leads to loss of pluripotency. It can be hypothesised that the loss of NUP205, like lamins, is likely to decrease the pluripotency of the NT2/D1 cells.

Figure 10

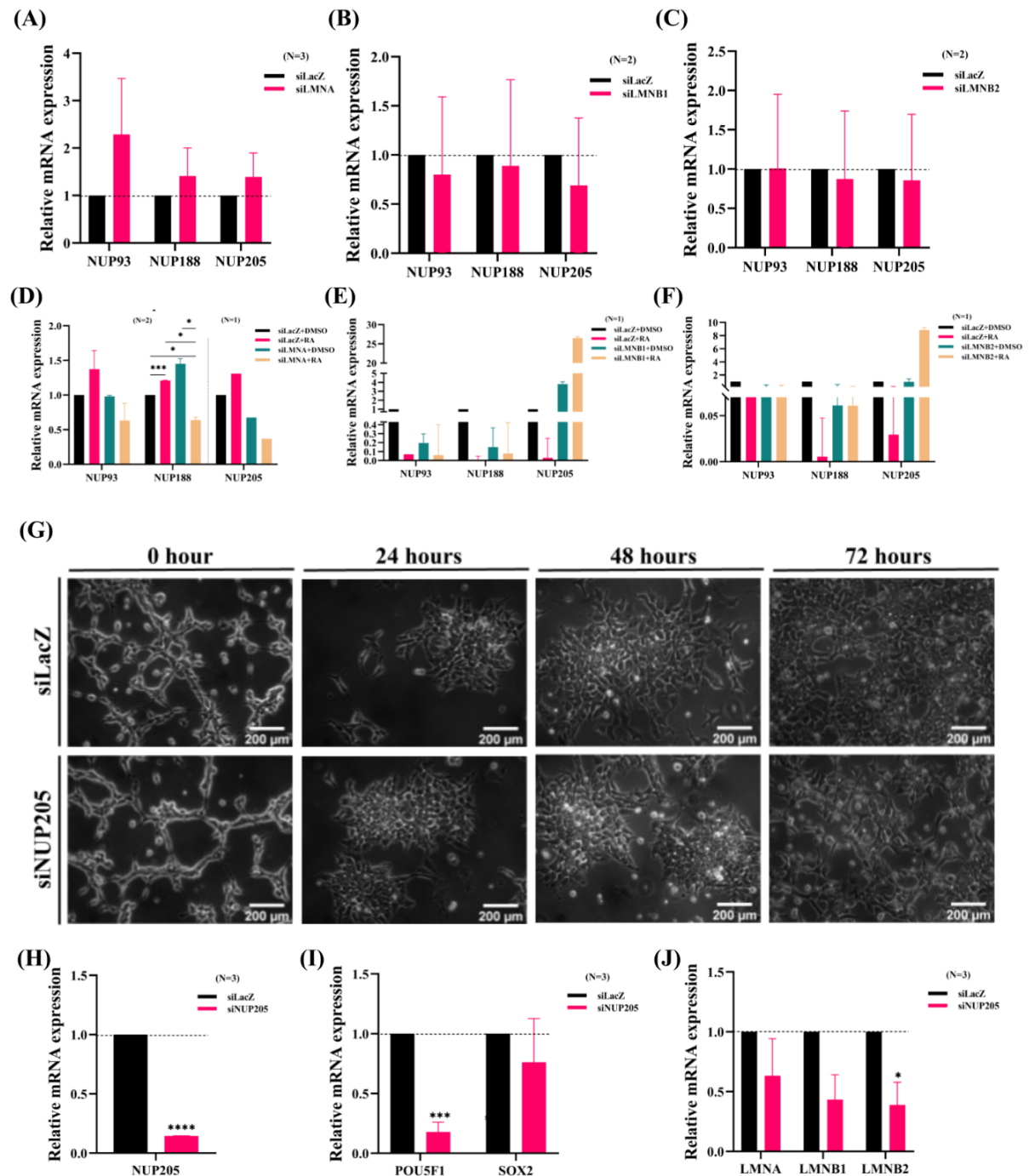


Fig. 10: Loss of lamins and NUP93-subcomplex proteins affect the expression levels of each other and the cellular pluripotency. (A-C) Transcript levels of NUP93-subcomplex proteins in cells with (A) Lamin A (N=3, n=9), (B) Lamin B1 (N=2, n=6), and (C) Lamin B2 (N=2, n=6) knock-down. (D-F) Transcript levels of NUP93-subcomplex proteins upon 8-days of differentiation in (D) Lamin A (N=3, n=9), (E) Lamin B1 (N=1, n=3), and (F) Lamin B2 (N=1, n=3) depleted cells. (G) Representative bright-field images showing qualitative changes in cell density and shape during 72 hours of siRNA-mediated knock-down of NUP205. (H) RT-qPCR levels of NUP205 validate the knock-down. (I-J) Transcript levels of (I) pluripotency markers and (J) lamins upon NUP205 knock-down. (N=3, n=9). Error bars represent the standard error of the mean.

3.7 Loss of either Lamin A and NUP205 affect the levels of the other during the initial stage of NT2/D1 differentiation.

It was earlier speculated that Lamin A might be dispensable in the early stages of differentiation while it might be required more during the later stages as compared to the B-type lamins (Fig. 6). To further explore this speculation, a short 4-day course of RA treatment was employed to study the levels of Lamins A and B1 with and without depletion of Lamin A during the initial stages of differentiation. NUP205, having been established as a consistent regulator of lamin expression, was also used to study the effect of its depletion on lamin levels upon 4 days of RA treatment. Using single-cell level protein quantification by IFA (Fig. 11A), it was observed that in the initial stage of differentiation (day 4), Lamin B1 levels were higher than Lamin A levels in the control cells, while both Lamin A and Lamin B1 levels slightly decreased upon differentiation (Fig. 11B). This is consistent with our earlier hypothesis that differentiation proceeds with a decrease in lamins and also indicates that Lamin A levels indeed are less than that of B-type lamins during the initial stages of differentiation.

In the case of NUP205 knock-down, both Lamin A and Lamin B1 levels were slightly higher than that of the control samples and the levels further increased with differentiation (Fig. 11B). This is contrary to the earlier observation where all lamins decrease upon loss of NUP205 at the transcript level (Fig. 10). This observation can be attributed to the fact that NUP205 being a relatively large protein might show a faster response to the siRNA-mediated knock-down at the transcript level while a longer transfection period or a higher dose of siRNA might be required for the knock-down to efficiently reflect at the protein level and hence, on its downstream regulatory activity.

Figure 11

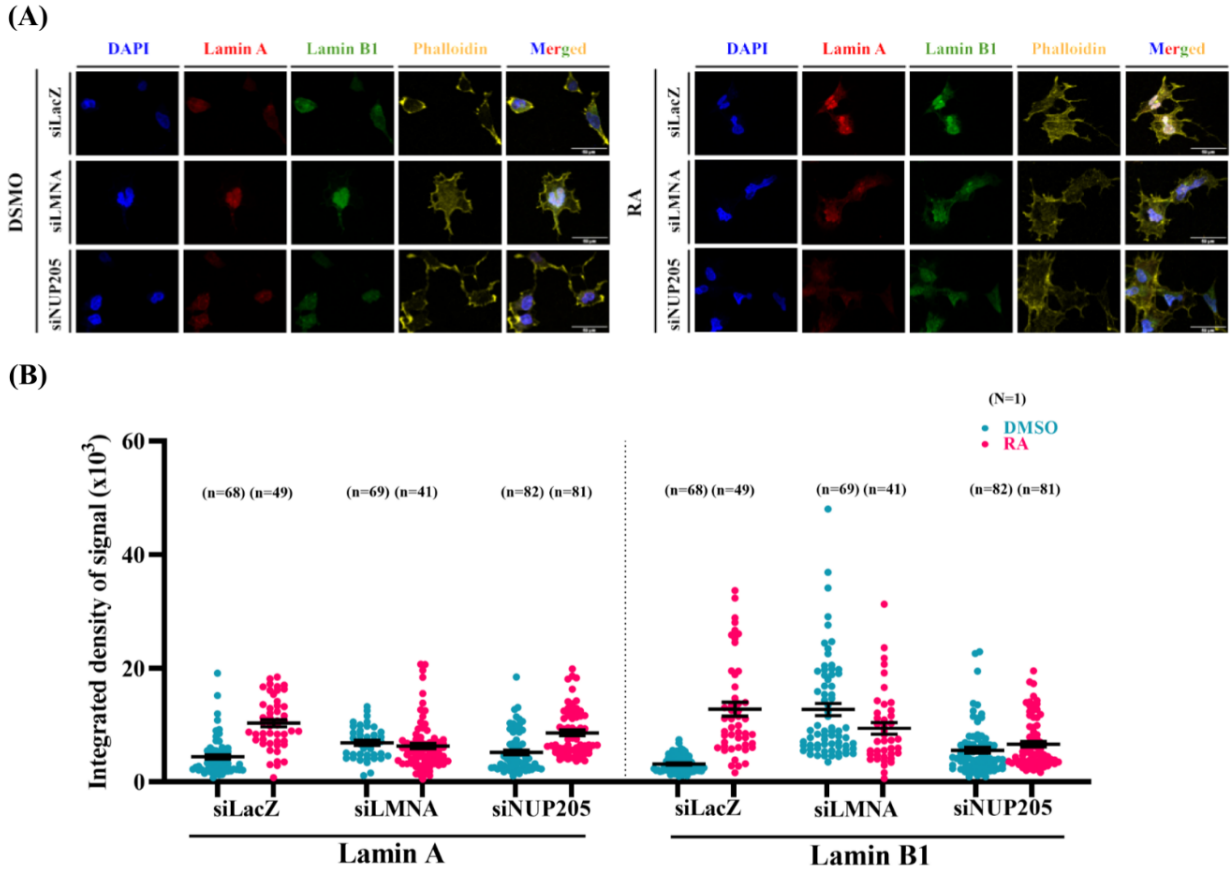


Fig. 11: Differentiation is affected by the loss of Lamin A and NUP205. (A) Representative images of immunofluorescence-stained Lamin A and Lamin B1 at the single-cell level in 4-day differentiated cells with loss of Lamin A and NUP205. (B) Single-cell protein expression of Lamin A and Lamin B1 in LMNA and NUP205-depleted cells. (N=1, n=~40-80, as shown in plot). Error bars represent the standard error of the mean.

4. Discussion

In this study, we successfully characterise the RA-mediated neuronal differentiation in NT2/D1 cells by validating the downregulated levels of the pluripotency factors *POU5F1*, *SOX2* and *NANOG* (>90%) and the upregulated levels of neuronal developmental marker *PAX6* (~500%) in cells after 8 days of RA treatment (Labade et al., 2021; Sansom et al., 2009). We also show that both the cellular and nuclear area increase upon differentiation, which is associated with the altered gene expression of the nuclear envelope proteins (Fig. E2).

Nuclear lamins are major components of the nuclear membrane. Owing to their localisation largely in the inner nuclear membrane and sometimes even in the nucleoplasm (Naetar et al., 2017), they associate with the genomic material in regions known as the lamin-associated domains (LADs) (Briand and Collas, 2020), and regulate chromatin supercoiling into heterochromatin, thus silencing the associated geneic regions (Popova et al. 2021; Wu and Yao, 2017). Cell fate transitions involve massive rearrangement in epigenetically-driven

expression profiles, and lamins have been understood to significantly affect this process ([Malashicheva and Perepelina, 2021](#); [Van Bortle and Corces, 2013](#)), with overarching effects on development and disease ([Paul and Fulka, 2022](#); [Zuela et al., 2012](#)). In the case of differentiation of pluripotent stem cells or multipotent precursor cells into specialised cells, lamins have been shown to either be upregulated or downregulated during the initiation and progression of differentiation depending on the cell type and lineage. For instance, mesenchymal stem cells differentiate into osteoblasts when Lamin A is upregulated but differentiate into adipocytes instead when lamins are downregulated ([Alcorta-Sevillano et al., 2020](#)). There is little clarity regarding the basis of cell or tissue-type specific differentiation when it comes to lamin expression and regulation. Moreover, a lot of studies have focussed on the role of Lamin A in differentiation and although a number of recent studies have revealed the role of B-type lamins during differentiation, it is crucial to understand the cumulative effects of both subtypes of lamins in a given system so as to have a clearer understanding of how the A-type lamins and B-type lamins interact with one another to modulate specific cellular identities together.

In this study, we have looked at all three lamin subtypes together and have frequently categorised our observations based on A-type lamins and B-types since Lamin B1 and Lamin B2 appear to have similar trends in expression and effect across most of the experiments performed. We find that both A-type lamins and B-type lamins are required for maintaining the pluripotency of the NT2/D1 cells and loss of lamins, specially the B-type lamins could possibly prime the cells for neuronal differentiation. We also see that although both lamins play a role in facilitating differentiation, B-type lamins are consistently upregulated in the initial as well as later stages of differentiation while Lamin A is expressed relatively more in the later stages of our differentiation duration, indicating that Lamin A is likely to be dispensable in the earlier stages and is crucial for the final stages of NT2/D1 differentiation. Alternatively, this can also be interpreted as depletion of Lamin A in the initial stages being necessary for the NT2/D1 cells to lose their pluripotency and differentiate. This is contrary to a number of existing studies which have reported that Lamin A overexpression is necessary for differentiation ([Nardella et al., 2015](#); [Wu et al., 2009](#); [Constantinescu et al., 2006](#)), again pointing towards the cell type and tissue-specific role of lamins during differentiation. Additionally, the temporal-specific regulation of the lamins is also crucial to note in this case since the differentiation strategy adopted in this study (8-10 days of RA treatment) does not lead to a terminal differentiation of neuronal cells whereas the earlier studies reported in the literature for RA differentiation of NT2/D1 cells follow a more long-term treatment of the cells by prolonged RA treatment ([Pierce et al., 1999](#); [Coyle et al., 2011](#); [Klajn et al., 2014](#)). It is possible that the Lamin A expression decreases towards the terminal stages in the differentiation based on the specific Lamin A-driven transcriptomic regulation required by the specific developmental stage of the neuron. We also find that Lamin A and Lamin B1 have indirect associations with pluripotency specific genes while Lamin B2 does not show such interactions but it directly interacts with Lamin A and Lamin B1.

When it comes to the effect of loss of a lamin subtype, we conclude that there is no lethality in the cells upon depletion of any of the lamin subtypes individually. We observe that B-type lamins are not considerably affected by the loss of Lamin A, whereas loss of either of the

B-type lamins is potentially compensated for by an increased expression of the other B-type lamin while Lamin A is significantly reduced with the loss of either of the B-type lamins, indicating that B-type lamins are necessary for the expression of *LMNA* but Lamin A may not be necessary for the expression of *LMNB1* or *LMNB2*. This is also in accordance with observations made in earlier studies that B-type lamins are expressed in most cell types and stages while Lamin A is expressed based on the developmental stage (Rober et al. 1989; Lin and Worman, 1995). The possible compensation in the transcript expression levels in the B-type lamins could be owing to the fact that Lamin B1 and Lamin B2 are very similar in their sequence, amino acid composition and structure, which is indicative of a possibility of their functional similarity as well (Lee et al., 2014). Earlier reports in the literature have also suggested the presence of functional redundancy in lamins, majorly for the B-type lamins (Lee et al., 2014; Camps et al., 2015; Comai, 2016) but a few studies have also investigated the functional compensation between A-type lamins and B-type lamins in *Drosophila* (Lenz-Böhme et al., 1997; Osouda et al., 2005). Lamins are critical proteins responsible for a number of important functions in the cell and although they are understood to have distinct functions, all the lamin subtypes come together to form the filamentous meshwork that underlies the nuclear membrane and contributes to its stability as well as regulates nucleo-cytoplasmic transport and thus transcription and translation by altering the NPC structures. Lamins also regulate genomic material packaging and gene expression by direct association with the chromatin. In the case that the loss of one lamin subtype prevents the optimal functioning and regulation of the cellular homeostasis and development, it is likely that another lamin subtype with a similar functionality is upregulated by a transcriptional feedback mechanism to compensate for the loss of function in the overall lamin network

We also show that all the Nups of the NUP93-complex (NUP93, NUP188, NUP205) help in maintaining pluripotency and when downregulated, prime the cells for differentiation like lamins. Also, the loss of any of the three lamins downregulates all the three Nups. We also observe that NUP205 has a stronger correlation with the levels of B-type lamins, and they indeed have a weak protein-protein association (Fig. 12). Upon loss of NUP205, Lamin A gets downregulated but B-type lamins get upregulated.

Figure 12

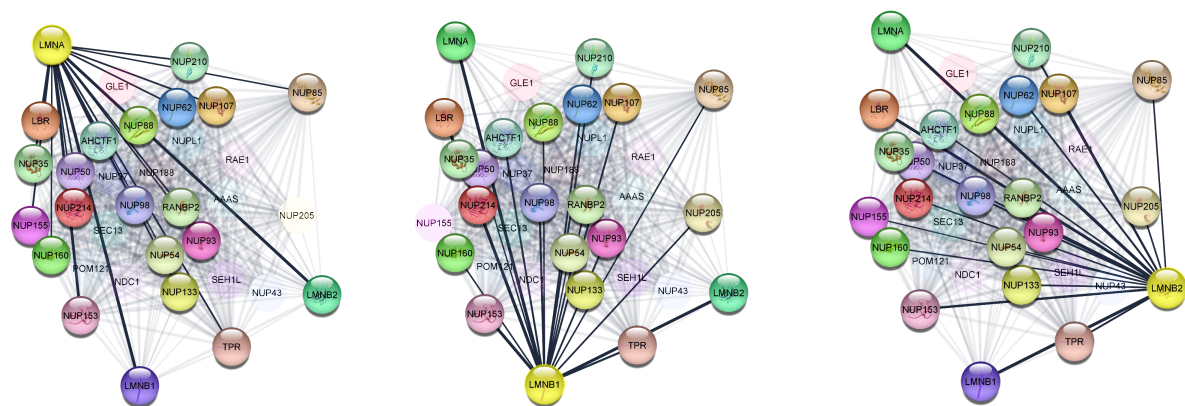


Fig. 12: Lamins interact with nucleoporins. Lamin B1 and Lamin B2 have a weak interaction with NUP205 while Lamin A associates with Nups from other NPCs.

5. Conclusion

Taken together, our data suggests that both A and B-type lamins are crucial for cellular differentiation in NT2/D1 cells but they are expressed in a temporally differential manner throughout the progression of the differentiation. Lamin B1 and B2 are consistently required throughout the initiation and progression of differentiation while Lamin A is more crucial for differentiation during the later stages of the process. We conclude that lamins in the NT2/D1 system are necessary for the maintenance of the pluripotent status of these cells and the loss of lamins results in loss of pluripotency. Similarly, NUP205 works in tandem with the B-type lamins to facilitate early differentiation in the NT2/D1 cells.

6. Future perspectives

Based on the observations from the correlational data between the lamins and the cell fate determinants, a ChIP-seq based analysis of the occupancy of each of the lamin subtypes in the loss of background of each other would help reveal a more mechanistic understanding of how the different lamins regulate the maintenance of pluripotency and differentiation in the NT2/D1 cells. A co-immunoprecipitation based approach should also be taken to validate the interaction between NUP205 and the B-type lamins during the course of differentiation in a temporal manner.

Although some of the experimental analyses in this study could be concluded with statistical significance, many experimental results show variation between replicates, limiting reproducibility in observations owing to the highly heterogeneous nature of a delicate pluripotent system like NT2/D1 which is very sensitive to minute changes in the growth and maintenance conditions. Additionally, since the NT2/D1 cells differentiate into a number of cell types in the neuro-ectodermal lineage initially and become post-mitotic neurons after 21 days of differentiation, the earlier stages have considerable population-level noise that skew the data reproducibility. For further experiments, the cells can be mitotically synchronised before experimentation in order to reduce the population level heterogeneity.

7. References

1. Agrawal, Ashutosh, and Tanmay P Lele. 2019. "Mechanics of Nuclear Membranes." *J. Cell Sci.* 132 (14). <https://doi.org/10.1242/jcs.229245>.
2. Alcorta-Sevillano, Natividad, Iratxe Macías, Clara I Rodríguez, and Arantza Infante. 2020. "Crucial Role of Lamin A/C in the Migration and Differentiation of MSCs in Bone." *Cells* 9 (6): 1330. <https://doi.org/10.3390/cells9061330>.
3. Alpsy, Aktan, Surbhi Sood, and Emily C Dykhuizen. 2021. "At the Crossroad of Gene Regulation and Genome Organization: Potential Roles for ATP-Dependent

- Chromatin Remodelers in the Regulation of CTCF-Mediated 3D Architecture.” *Biology* 10 (4). <https://doi.org/10.3390/biology10040272>.
4. Andrés, Vicente, and José M González. 2009. “Role of A-Type Lamins in Signaling, Transcription, and Chromatin Organization.” *J. Cell Biol.* 187 (7): 945–57. <https://doi.org/10.1083/jcb.200904124>.
 5. Baldassarre, G, A Boccia, P Bruni, C Sandomenico, M V Barone, S Pepe, T Angrisano, et al. 2000. “Retinoic Acid Induces Neuronal Differentiation of Embryonal Carcinoma Cells by Reducing Proteasome-Dependent Proteolysis of the Cyclin-Dependent Inhibitor P27.” *Cell Growth Differ.* 11 (10): 517–26.
 6. Bedrosian, Tracy A, Judith Houtman, Juan Sebastian Eguiguren, Saeed Ghassemzadeh, Nicole Rund, Nicole M Novaresi, Lauren Hu, et al. 2021. “Lamin B1 Decline Underlies Age-Related Loss of Adult Hippocampal Neurogenesis.” *EMBO J.* 40 (3): e105819. <https://doi.org/10.15252/embj.2020105819>.
 7. Briand, Nolwenn, and Philippe Collas. 2020. “Lamina-Associated Domains: Peripheral Matters and Internal Affairs.” *Genome Biol.* 21 (1): 85. <https://doi.org/10.1186/s13059-020-02003-5>.
 8. Camps, Jordi, Michael R. Erdos, and Thomas Ried. 2015. “The Role of Lamin B1 for the Maintenance of Nuclear Structure and Function.” *Nucleus* 6 (1): 8–14.
 9. Caricasole, A, D Ward-van Oostwaard, L Zeinstra, A van den Eijnden-van Raaij, and C Mummery. 2000. “Bone Morphogenetic Proteins (BMPs) Induce Epithelial Differentiation of NT2D1 Human Embryonal Carcinoma Cells.” *Int. J. Dev. Biol.* 44 (5): 443–50.
 10. Chadalavada, Rajendrakumar S V, Jane Houldsworth, Adam B Olshen, George J Bosl, Lorenz Studer, and R S K Chaganti. 2005. “Transcriptional Program of Bone Morphogenetic Protein-2-Induced Epithelial and Smooth Muscle Differentiation of Pluripotent Human Embryonal Carcinoma Cells.” *Funct. Integr. Genomics* 5 (2): 59–69. <https://doi.org/10.1007/s10142-005-0132-7>.
 11. Comai, Lucio. 2016. “Faculty Opinions Recommendation of Reciprocal Knock-in Mice to Investigate the Functional Redundancy of Lamin B1 and Lamin B2.” *Faculty Opinions – Post-Publication Peer Review of the Biomedical Literature*. <https://doi.org/10.3410/f.718325527.793523830>.
 12. Constantinescu, Dan, Heather L Gray, Paul J Sammak, Gerald P Schatten, and Antonei B Csoka. 2006. “Lamin A/C Expression Is a Marker of Mouse and Human Embryonic Stem Cell Differentiation.” *Stem Cells* 24 (1): 177–85. <https://doi.org/10.1634/stemcells.2004-0159>.
 13. Coutinho, Henrique Douglas M, Vivyanne S Falcão-Silva, Gregório Fernandes Gonçalves, and Raphael Batista da Nóbrega. 2009. “Molecular Ageing in Progeroid Syndromes: Hutchinson-Gilford Progeria Syndrome as a Model.” *Immun. Ageing* 6 (April): 4. <https://doi.org/10.1186/1742-4933-6-4>.
 14. Coyle, Dennis E, Jie Li, and Mark Baccei. 2011. “Regional Differentiation of Retinoic Acid-Induced Human Pluripotent Embryonic Carcinoma Stem Cell Neurons.” *PLoS One* 6 (1): e16174. <https://doi.org/10.1371/journal.pone.0016174>.
 15. Crispatzu, Giuliano, Rizwan Rehimi, Tomas Pachano, Tore Bleckwehl, Sara Cruz-Molina, Cally Xiao, Esther Mahabir, Hisham Bazzi, and Alvaro Rada-Iglesias.

2021. “The Chromatin, Topological and Regulatory Properties of Pluripotency-Associated Poised Enhancers Are Conserved in Vivo.” *Nat. Commun.* 12 (1): 4344. <https://doi.org/10.1038/s41467-021-24641-4>.
16. Dorner, Daniela, Josef Gotzmann, and Roland Foisner. 2007. “Nucleoplasmic Lamins and Their Interaction Partners, LAP2 α , Rb, and BAF, in Transcriptional Regulation.” *FEBS J.* 274 (6): 1362–73. <https://doi.org/10.1111/j.1742-4658.2007.05695.x>.
17. Ghosh, Arindam, and Anup Som. 2020. “RNA-Seq Analysis Reveals Pluripotency-Associated Genes and Their Interaction Networks in Human Embryonic Stem Cells.” *Comput. Biol. Chem.* 85 (April): 107239. <https://doi.org/10.1016/j.compbiolchem.2020.107239>.
18. Heo, Su-Jin, Tristan P Driscoll, Stephen D Thorpe, Nandan L Nerurkar, Brendon M Baker, Michael T Yang, Christopher S Chen, David A Lee, and Robert L Mauck. 2016. “Differentiation Alters Stem Cell Nuclear Architecture, Mechanics, and Mechano-Sensitivity.” *Elife* 5 (November). <https://doi.org/10.7554/eLife.18207>.
19. Ikeda, Hiroki, Masamitsu Sone, Shinya Yamanaka, and Takuya Yamamoto. 2017. “Structural and Spatial Chromatin Features at Developmental Gene Loci in Human Pluripotent Stem Cells.” *Nat. Commun.* 8 (1): 1616. <https://doi.org/10.1038/s41467-017-01679-x>.
20. Khan, Asmat Ullah, Rongmei Qu, Jun Ouyang, and Jingxing Dai. 2020. “Role of Nucleoporins and Transport Receptors in Cell Differentiation.” *Front. Physiol.* 11 (April): 239. <https://doi.org/10.3389/fphys.2020.00239>.
21. Klajn, A., D. Drakulic, M. Tosic, Z. Pavkovic, M. Schwirtlich, and M. Stevanovic. 2014. “SOX2 Overexpression Affects Neural Differentiation of Human Pluripotent NT2/D1 Cells.” *Biochemistry. Biokhimiia* 79 (11): 1172–82.
22. Kleinsmith, L J, and G B Pierce Jr. 1964. “MULTIPOTENTIALITY OF SINGLE EMBRYONAL CARCINOMA CELLS.” *Cancer Res.* 24 (October): 1544–51.
23. Labade, Ajay S, Adwait Salvi, Saswati Kar, Krishanpal Karmodiya, and Kundan Sengupta. 2021. “Nup93 and CTCF Modulate Spatiotemporal Dynamics and Function of the HOXA Gene Locus during Differentiation.” *J. Cell Sci.* 134 (23). <https://doi.org/10.1242/jcs.259307>.
24. Lee, John M., Hea-Jin Jung, Loren G. Fong, and Stephen G. Young. 2014. “Do Lamin B1 and Lamin B2 Have Redundant Functions?” *Nucleus* 5 (4): 287–92.
25. Lenz-Böhme, Bettina, Jasmine Wismar, Silke Fuchs, Rita Reifegerste, Erich Buchner, Heinrich Betz, and Bertram Schmitt. 1997. “Insertional Mutation of the Drosophila Nuclear Lamin Dm0 Gene Results in Defective Nuclear Envelopes, Clustering of Nuclear Pore Complexes, and Accumulation of Annulate Lamellae.” *Journal of Cell Biology.* <https://doi.org/10.1083/jcb.137.5.1001>.
26. Lin, F, and H J Worman. 1995. “Structural Organization of the Human Gene (LMNB1) Encoding Nuclear Lamin B1.” *Genomics* 27 (2): 230–36. <https://doi.org/10.1006/geno.1995.1036>.
27. Livak, Kenneth J, and Thomas D Schmittgen. 2001. “Analysis of Relative Gene Expression Data Using Real-Time Quantitative PCR and the 2- $\Delta\Delta$ CT Method.” *Methods* 25 (4): 402–8.

28. Lourim, D., and J. J. Lin. 1992. "Expression of Wild-Type and Nuclear Localization-Deficient Human Lamin A in Chick Myogenic Cells." *Journal of Cell Science* 103 (Pt 3) (November): 863–74.
29. Lusk, C Patrick, and Megan C King. 2017. "The Nucleus: Keeping It Together by Keeping It Apart." *Curr. Opin. Cell Biol.* 44 (February): 44–50. <https://doi.org/10.1016/j.ceb.2017.02.001>.
30. Mahajani, Sameehan, Caterina Giacomini, Federica Marinaro, Davide De Pietri Tonelli, Andrea Contestabile, and Laura Gasparini. 2017. "Lamin B1 Levels Modulate Differentiation into Neurons during Embryonic Corticogenesis." *Sci. Rep.* 7 (1): 4897. <https://doi.org/10.1038/s41598-017-05078-6>.
31. Maire, Albane le, Catherine Teyssier, Patrick Balaguer, William Bourguet, and Pierre Germain. 2019. "Regulation of RXR-RAR Heterodimers by RXR- and RAR-Specific Ligands and Their Combinations." *Cells* 8 (11). <https://doi.org/10.3390/cells8111392>.
32. Malashicheva, Anna, and Kseniya Perepelina. 2021. "Diversity of Nuclear Lamin A/C Action as a Key to Tissue-Specific Regulation of Cellular Identity in Health and Disease." *Front Cell Dev Biol* 9 (October): 761469. <https://doi.org/10.3389/fcell.2021.761469>.
33. Marei, Hany E, A Althani, S Lashen, C Cenciarelli, and Anwarul Hasan. 2017. "Genetically Unmatched Human iPSC and ESC Exhibit Equivalent Gene Expression and Neuronal Differentiation Potential." *Sci. Rep.* 7 (1): 17504. <https://doi.org/10.1038/s41598-017-17882-1>.
34. Marmiroli, Sandra, Jessika Bertacchini, Francesca Beretti, Vittoria Cenni, Marianna Guida, Anto De Pol, Nadir M Maraldi, and Giovanna Lattanzi. 2009. "A-Type Lamins and Signaling: The PI 3-Kinase/Akt Pathway Moves Forward." *J. Cell. Physiol.* 220 (3): 553–61. <https://doi.org/10.1002/jcp.21807>.
35. McPherson, Annie J, Allison Lange, Paul W Doetsch, and Anita H Corbett. 2015. "Nuclear–Cytoplasmic Transport," March, 1–9. <https://doi.org/10.1002/9780470015902.a0001351.pub3>.
36. Naetar, Nana, Simona Ferraioli, and Roland Foisner. 2017. "Lamins in the Nuclear Interior – Life Outside the Lamina." *Journal of Cell Science* 130 (13): 2087–96. <https://doi.org/10.1242/jcs.203430>.
37. Nardella, Marta, Loredana Guglielmi, Carla Musa, Ilaria Iannetti, Giovanna Maresca, Donatella Amendola, Manuela Porru, et al. 2015. "Down-Regulation of the Lamin A/C in Neuroblastoma Triggers the Expansion of Tumor Initiating Cells." *Oncotarget* 6 (32): 32821–40. <https://doi.org/10.18632/oncotarget.5104>.
38. Okumura, K, K Nakamachi, Y Hosoe, and N Nakajima. 2000. "Identification of a Novel Retinoic Acid-Responsive Element within the Lamin A/C Promoter." *Biochem. Biophys. Res. Commun.* 269 (1): 197–202. <https://doi.org/10.1006/bbrc.2000.2242>.
39. Osouda, Shinichi, Yoshihiro Nakamura, Brigitte de Saint Phalle, Maeve McConnell, Tsuneyoshi Horigome, Shin Sugiyama, Paul A. Fisher, and Kazuhiro Furukawa. 2005. "Null Mutants of Drosophila B-Type Lamin Dm0 Show Aberrant Tissue Differentiation rather than Obvious Nuclear Shape Distortion or Specific Defects during Cell Proliferation." *Developmental Biology.* <https://doi.org/10.1016/j.ydbio.2005.05.022>.

40. Patil, Shalaka, and Kundan Sengupta. 2021. "Role of A- and B-Type Lamins in Nuclear Structure-Function Relationships." *Biol. Cell* 113 (7): 295–310. <https://doi.org/10.1111/boc.202000160>.
41. Paul, Jasper Chrysolite, and Helena Fulka. 2022. "Nuclear Lamins: Key Proteins for Embryonic Development." *Biology* 11 (2). <https://doi.org/10.3390/biology11020198>.
42. Pierce, T., H. J. Worman, and J. Holy. 1999. "Neuronal Differentiation of NT2/D1 Teratocarcinoma Cells Is Accompanied by a Loss of Lamin A/C Expression and an Increase in Lamin B1 Expression." *Experimental Neurology* 157 (2): 241–50.
43. Pleasure, S J, and V M Lee. 1993. "NTERA 2 Cells: A Human Cell Line Which Displays Characteristics Expected of a Human Committed Neuronal Progenitor Cell." *J. Neurosci. Res.* 35 (6): 585–602. <https://doi.org/10.1002/jnr.490350603>.
44. Popova, Liudmila V, Prabakaran Nagarajan, Callie M Lovejoy, Benjamin D Sunkel, Miranda L Gardner, Meng Wang, Michael A Freitas, Benjamin Z Stanton, and Mark R Parthun. 2021. "Epigenetic Regulation of Nuclear Lamina-Associated Heterochromatin by HAT1 and the Acetylation of Newly Synthesized Histones." *Nucleic Acids Res.* 49 (21): 12136–51. <https://doi.org/10.1093/nar/gkab1044>.
45. Raices, Marcela, and Maximiliano A D'Angelo. 2022. "Structure, Maintenance, and Regulation of Nuclear Pore Complexes: The Gatekeepers of the Eukaryotic Genome." *Cold Spring Harb. Perspect. Biol.* 14 (3). <https://doi.org/10.1101/cshperspect.a040691>.
46. Rapley, Elizabeth A, Clare Turnbull, Ali Amin Al Olama, Emmanouil T Dermitzakis, Rachel Linger, Robert A Huddart, Anthony Renwick, et al. 2009. "A Genome-Wide Association Study of Testicular Germ Cell Tumor." *Nat. Genet.* 41 (7): 807–10. <https://doi.org/10.1038/ng.394>.
47. Rio, Donald C, Manuel Ares Jr, Gregory J Hannon, and Timothy W Nilsen. 2010. "Purification of RNA Using TRIzol (TRI Reagent)." *Cold Spring Harb. Protoc.* 2010 (6): db.prot5439. <https://doi.org/10.1101/pdb.prot5439>.
48. Rober, R A, K Weber, and M Osborn. 1989. "Differential Timing of Nuclear Lamin A/C Expression in the Various Organs of the Mouse Embryo and the Young Animal: A Developmental Study." *Development* 105 (2): 365–78. <https://doi.org/10.1242/dev.105.2.365>.
49. Rochette-Egly, Cécile. 2015. "Retinoic Acid Signaling and Mouse Embryonic Stem Cell Differentiation: Cross Talk between Genomic and Non-Genomic Effects of RA." *Biochim. Biophys. Acta* 1851 (1): 66–75. <https://doi.org/10.1016/j.bbali.2014.04.003>.
50. Sansom, Stephen N, Dean S Griffiths, Andrea Faedo, Dirk-Jan Kleinjan, Youlin Ruan, James Smith, Veronica van Heyningen, John L Rubenstein, and Frederick J Livesey. 2009. "The Level of the Transcription Factor Pax6 Is Essential for Controlling the Balance between Neural Stem Cell Self-Renewal and Neurogenesis." *PLoS Genet.* 5 (6): e1000511. <https://doi.org/10.1371/journal.pgen.1000511>.
51. Schindelin, Johannes, Ignacio Arganda-Carreras, Erwin Frise, Verena Kaynig, Mark Longair, Tobias Pietzsch, Stephan Preibisch, et al. 2012. "Fiji: An Open-Source Platform for Biological-Image Analysis." *Nat. Methods* 9 (7): 676–82. <https://doi.org/10.1038/nmeth.2019>.

52. Simões, Pedro D., and Teresa Ramos. 2007. "Human Pluripotent Embryonal Carcinoma NTERA2 cl.D1 Cells Maintain Their Typical Morphology in an Angiomyogenic Medium." *Journal of Negative Results in BioMedicine*. <https://doi.org/10.1186/1477-5751-6-5>.
53. Smith, Cheryl L, Andrey Poleshko, and Jonathan A Epstein. 2021. "The Nuclear Periphery Is a Scaffold for Tissue-Specific Enhancers." *Nucleic Acids Res.* 49 (11): 6181–95. <https://doi.org/10.1093/nar/gkab392>.
54. Sumner, Michael Chas, and Jason Brickner. 2022. "The Nuclear Pore Complex as a Transcription Regulator." *Cold Spring Harb. Perspect. Biol.* 14 (1). <https://doi.org/10.1101/cshperspect.a039438>.
55. Van Bortle, Kevin, and Victor G Corces. 2013. "Spinning the Web of Cell Fate." *Cell* 152 (6): 1213–17. <https://doi.org/10.1016/j.cell.2013.02.052>.
56. Wilson, Rachel, Afsara A Ahmmed, Alistair Poll, Motoharu Sakaue, Alex Laude, and Maya Sieber-Blum. 2018. "Human Peptidergic Nociceptive Sensory Neurons Generated from Human Epidermal Neural Crest Stem Cells (HEPI-NCSC)." *PLoS One* 13 (6): e0199996. <https://doi.org/10.1371/journal.pone.0199996>.
57. Wu, Feinan, and Jie Yao. 2017. "Identifying Novel Transcriptional and Epigenetic Features of Nuclear Lamina-Associated Genes." *Sci. Rep.* 7 (1): 100. <https://doi.org/10.1038/s41598-017-00176-x>.
58. Wu, Zhengrong, Lirong Wu, Desheng Weng, Dazhi Xu, Jian Geng, and Fei Zhao. 2009. "Reduced Expression of Lamin A/C Correlates with Poor Histological Differentiation and Prognosis in Primary Gastric Carcinoma." *J. Exp. Clin. Cancer Res.* 28 (January): 8. <https://doi.org/10.1186/1756-9966-28-8>.
59. Xie, Wei, Alexandre Chojnowski, Thomas Boudier, John S Y Lim, Sohail Ahmed, Zheng Ser, Colin Stewart, and Brian Burke. 2016. "A-Type Lamins Form Distinct Filamentous Networks with Differential Nuclear Pore Complex Associations." *Curr. Biol.* 26 (19): 2651–58. <https://doi.org/10.1016/j.cub.2016.07.049>.
60. Yattah, Camila, Marylens Hernandez, Dennis Huang, Hyejin Park, Will Liao, and Patrizia Casaccia. 2020. "Dynamic Lamin B1-Gene Association During Oligodendrocyte Progenitor Differentiation." *Neurochem. Res.* 45 (3): 606–19. <https://doi.org/10.1007/s11064-019-02941-y>.
61. Zhang, Jiajun, Qing Nie, and Tianshou Zhou. 2019. "Revealing Dynamic Mechanisms of Cell Fate Decisions From Single-Cell Transcriptomic Data." *Front. Genet.* 10 (December): 1280. <https://doi.org/10.3389/fgene.2019.01280>.
62. Zhou, Xuemei, Zhenzhen Liu, Kun Shen, Peng Zhao, and Meng-Xiang Sun. 2020. "Cell Lineage-Specific Transcriptome Analysis for Interpreting Cell Fate Specification of Proembryos." *Nat. Commun.* 11 (1): 1366. <https://doi.org/10.1038/s41467-020-15189-w>.
63. Zuela, Noam, Daniel Z Bar, and Yosef Gruenbaum. 2012. "Lamins in Development, Tissue Maintenance and Stress." *EMBO Rep.* 13 (12): 1070–78. <https://doi.org/10.1038/embor.2012.167>.

8. Extended Methods

8.1 Quantification of lamins from single-cell IFA images

The mid-optical section or the section of maximum intensity was extracted from the z-stacks and stored in an input folder. An output folder for the quantified results was also defined. The algorithm in Fiji's IJM language used is attached here in this link:

[Lamins_quantification_IFA_batch_processing](#)

For merging all output data sets from each frame for a sample into a single .csv file, the following Linux-terminal based commands were used:

[Lamin_quantification_post-processing_merge](#)

9. Extended Results

Figure E1

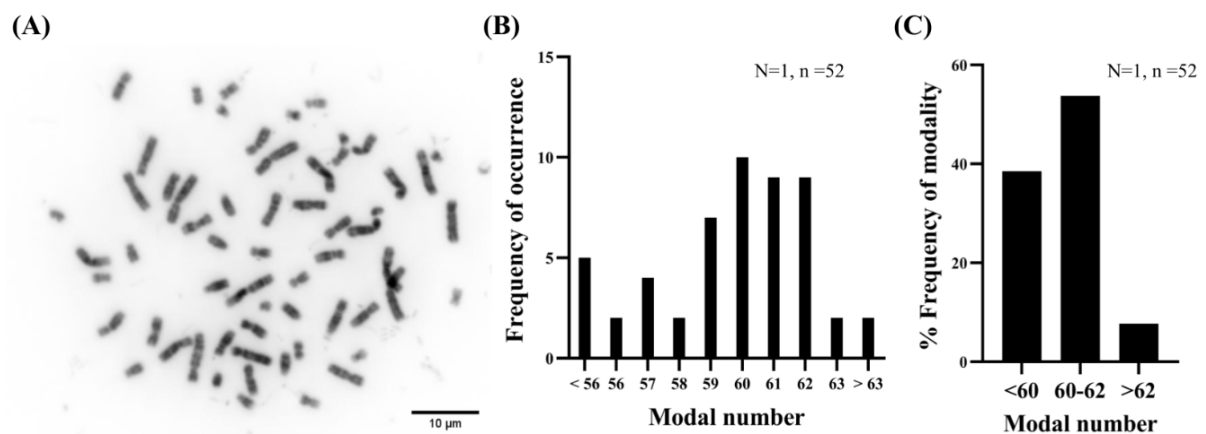


Fig. E1: NT2/D1 validation by karyotyping of fixed metaphases. (A) Representative image of the metaphase spread for NT2/D1 cells. (B) Quantification of how many times a specific number of chromosomes appear across the population (modal number). (C) Percentage of the population exhibiting the accepted modal number for NT2/D1.

Figure E2
(A)

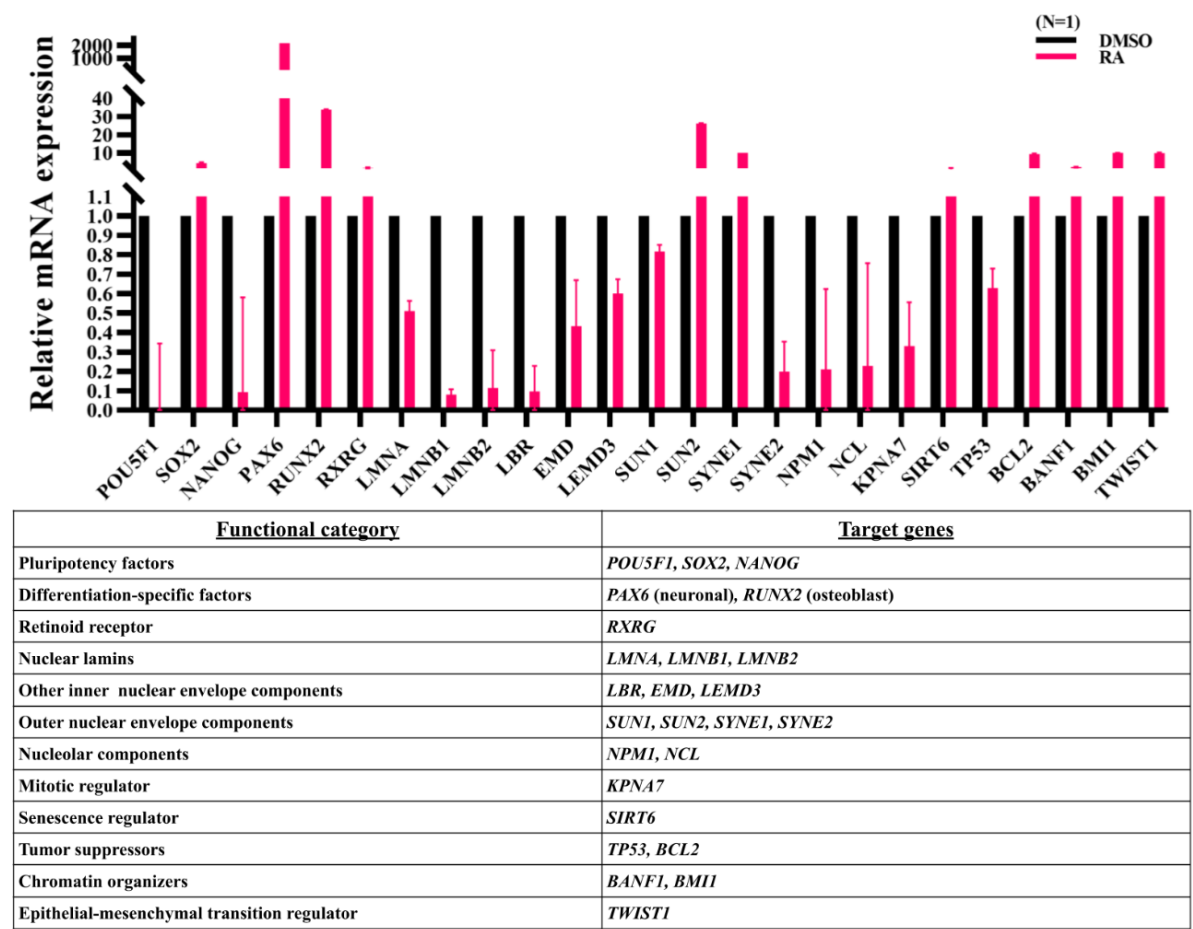


Fig. E2: Transcript levels of relevant nuclear proteins upon differentiation. (A) RT-qPCR levels of different nuclear envelope components, pluripotency and differentiation factors, and chromatin architecture regulators, by 10 days of RA treatment.

Figure E3

(A)

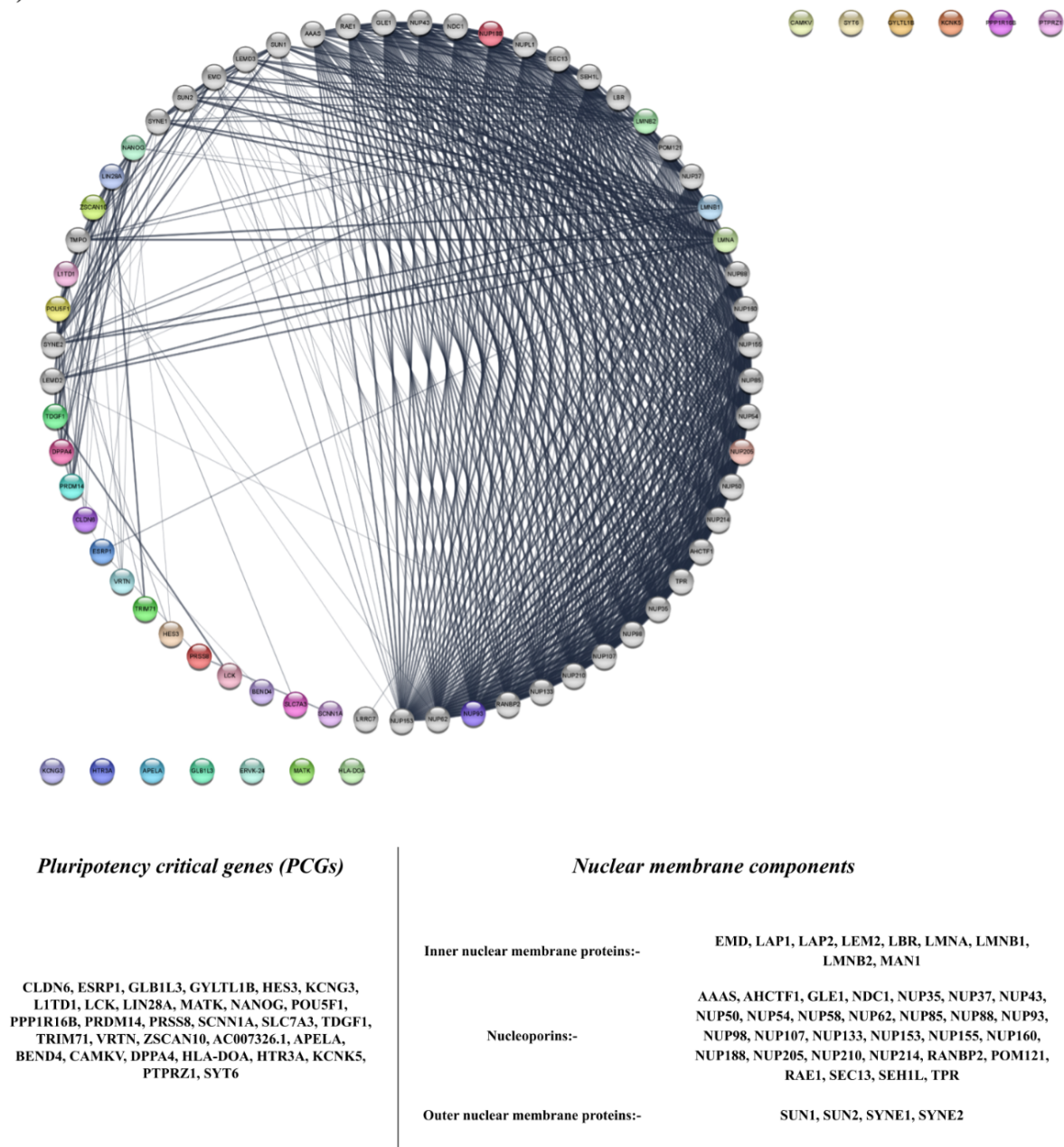


Fig. E3: An interaction network analysis of nuclear envelope proteins with pluripotency critical genes (PCGs). The different inner and outer nuclear membrane proteins (shown on the right side of the chart) have been mapped to known proteins critical for the maintenance of pluripotency (shown on the left side of the chart) based on the degree of protein-protein interaction. Thin lines represent weak or predictive associations while thick lines represent experimentally validated associations.